CO_2 FLUXES IN THE SOUTH AFRICAN COASTAL REGION

Veronica Arnone

Curso 2016/2017

Dr. Melchor González Dávila

Dra. J. Magdalena Santana Casiano

Trabajo Fin de Título para la obtención del título: Máster en Oceanografía

Master Interuniversitario en Oceanografía

FACULTAD DE CIENCIAS DEL MAR
UNIVERSIDAD DE LAS PALMAS DE GRAN CANARIA

QUIMA QUÍMICA MARINA ULPGC

IOCAG Instituto de Oceanografía y Cambio Global

CO_2 FLUXES IN THE SOUTH AFRICAN COASTAL REGION

Datos personales del estudiante:

Veronica Arnone

Máster Interuniversitario en Oceanografía

Curso 2016/2017

Universidad de Las Palmas de Gran Canaria, Facultad de Ciencias del Mar

Datos personales de los tutores:

Melchor González Dávila

Universidad de Las Palmas de Gran Canaria,

Facultad de Ciencias del Mar

Departamento de Química

J. Magdalena Santana Casiano

Universidad de Las Palmas de Gran Canaria,

Facultad de Ciencias del Mar

Departamento de Química

En Las Palmas de Gran Canaria, a.....7.....de.DICIEMBRE.....de 2016.

Estudiante: Veronica Arnone

Tutor: Dr. Melchor González Dávila

Co-tutora: Dra. J. Magdalena Santana Casiano

CONTENTS

Abstract 3

1. Introduction 4

1.1 The carbonate system in the ocean 4

1.2 South African Coastal Region 6

2. Material and methods 8

2.1 Temperature, salinity, and xCO_2 measurements 8

2.2 Determination of fugacity and fluxes of CO_2 9

2.3 Computational method 11

3. Results 12

3.1 Hydrographic situation 12

3.2 fCO_2 distribution and variability 14

3.3 CO_2 fluxes 15

3.4 Fits of harmonic functions 17

4. Discussion 20

4.1 Hydrographic situation 20

4.2 fCO_2 variability 21

4.3 FCO_2 over the coastal region 22

4.4 Seasonal and interannual trends 24

5. Conclusion 26

Acknowledgments 27

References 28

APPENDIX 29

Abstract

The air-sea exchange of CO_2, its distribution and trends in the South African continental shelf were described with measurement made using a volunteer observing ship (VOS) that operated along the QUIMA-VOS line over 6 years (2005-2008 and 2011-2012) and provided 30 journeys. Seawater properties, strongly controlled by oceanographic dynamic, showed a complex pattern of distribution between Cape Town and Durban. Three different upwelling cells were identified and dominated the regional variability, together with the presence of eddies, filaments and the core of Agulhas Current. From west to east the variation of fugacity (fCO_2) follows the temperature increase and the incorporation of South West Indian Central Water onto the shelf, resulting in oversaturated (>600 µatm) and undersaturated (~215 µatm) waters, affected by the presence of organisms that uptake CO_2. Seasonal and interannual cycles for SST, salinity, wind, fCO_2 and FCO_2 showed a longitudinal dependent trend. From 2005 to 2012, salinity, wind, fCO_2 and FCO_2 decreased while SST increased, the magnitude depending on the region.

From 18º25'E to 20º15'E (West Region) surface water was undersaturated and presented an averaged flux of -2.06 ± 2.10 mol m^{-2} yr^{-1}. For the South Region (20º15'E-28º30'E) a value of -2.33 ± 1.58 mol m^{-2} yr^{-1} is reached, while between 28º30'E and 31º15'E (East Region) the averaged flux is -1.19 ± 1.11 mol m^{-2} yr^{-1}. The studied area acted as a sink with a mean value of -2.04 ± 1.65 mol m^{-2} yr^{-1}. From Cape Town to Durban, between 2005 and 2012 and assuming that FCO_2 obtained with the harmonic fit was uniform over the shelf considered ($1490 \cdot 10^8$ m^2), the South African coastal region uptakes 3.66 ± 0.10 Tg C yr^{-1} with an interannual increase of 0.04 ± 0.10 Tg C yr^{-1}.

1. Introduction

1.1 The carbonate system in the ocean

The ocean plays an important role in the global carbon cycle, it controls atmospheric carbon dioxide (CO_2) content and ultimately the Earth's climate (Bates *et al.*, 2014; Herr & Galland, 2009). CO_2 represents one of the long-lived atmospheric greenhouse gases, it circulates between the atmosphere, ocean and terrestrial biosphere reservoirs on a broad range of timescales. Seawater acts as a buffer by absorbing and exchanging CO_2 through air-sea interface with significant implications for surface ocean chemistry, marine organisms and ecosystems (Bates *et al.*, 2014; Doney *et al.*, 2009; Orr *et al.*, 2005). The perturbation of the atmospheric CO_2 concentration and its increase is related to human activities, such as fossil fuel combustion, deforestation and land-use change (Le Quéré *et al.*, 2016). As described by different authors (Gruber *et al.*, 2009; Le Quéré *et al.*, 2016; Le Quéré *et al.*, 2015a; McKinley *et al.*, 2016; Sabine *et al.*, 2004; Sitch *et al.*, 2015; Takahashi *et al.*, 2009), on average, half of industrial emissions is taken up by the ocean (25 - 40%) and land (~30%), the rest of it remains in the atmosphere. Atmospheric CO_2 dissolution in seawater translates into a decrease in surface ocean pH due to the alteration of the equilibrium established between different inorganic carbon forms (carbonic acid [H_2CO_3], bicarbonate ion [HCO_3^-] and carbonate ion [CO_3^{2-}]):

$$CO_2(gas) \rightleftharpoons CO_2(aqueous) + H_2O \rightleftharpoons H_2CO_3 + H^+ \rightleftharpoons HCO_3^- + H^+ \rightleftharpoons CO_3^{2-} + H^+$$

Surface ocean pH ranges between 8.1 and 8.2, where HCO_3^- is the dominant form of inorganic carbon (Bates *et al.*, 2014; Doney *et al.*, 2009). Adding CO_2 to seawater leads to a reduction of carbonate ions and, in turn, to a decline in the saturation states (Ω) of calcium carbonate minerals (Bates *et al.*, 2014; Doney *et al.*, 2009; Orr *et al.*, 2005).

From the beginning of the industrial era to 2014 the content of carbon dioxide in the atmosphere has increased from 277 to 397.15 parts per million (ppm) (Le Quéré *et al.*, 2016; Le Quéré *et al.*, 2015a). In 1958, at Mauna Loa Observatory, Charles David Keeling began making daily measurements of atmospheric CO_2 concentration. This record being first in evidencing the clear rise of this gas and in May 2013 the daily mean surpassed, for the first time, the 400 ppm level (Le Quéré *et al.*, 2015a). Nowadays, international collaborative efforts try to make an accurate assessment of the carbon emissions, their redistribution among the major reservoir (Table I) and continuously update the global carbon budget (Le Quéré *et al.*, 2013; Le Quéré *et al.*, 2016; Le Quéré *et al.*, 2015a; Le Quéré *et al.*, 2015b) . In addition, international and intergovernmental programs make common effort for the assessment of climate change, to provide a scientific view on the current state of knowledge and its potential environmental and socio-economic impacts.

As reflected in the Synthesis Report of the Intergovernmental Panel on Climate Change (IPCC), actions that could stabilize climate are required to staying within 2ºC above pre-industrial conditions by 2100 (Fuss *et al.*, 2014; IPCC, 2014; Jackson *et al.*, 2015), the best future scenario.

Table 1. Decadal mean in the five components of the anthropogenic CO_2 budget for the periods 1960–1969, 1970–1979, 1980–1989, 1990–1999, 2000–2009, the last decade, and the last year available. All values are in GtC yr^{-1}. All uncertainties are reported as $\pm 1\sigma$. A data set containing data for each year during 1959–2014 is available at http://cdiac.ornl.gov/GCP/carbonbudget/2015/. Source: (Le Quéré *et al.*, 2016).

	Mean (GtC yr^{-1})						
	1960–1969	1970–1979	1980–1989	1990–1999	2000–2009	2005–2014	2014
Emissions							
Fossil fuels and industry	3.1 ±0.2	4.7 ±0.2	5.5 ±0.3	6.3 ±0.3	8.0 ±0.4	9.3 ±0.5	9.9 ±0.5
Land-use-change	1.5 ±0.5	1.3 ±0.5	1.4 ±0.5	1.6 ±0.5	1.0 ±0.5	1.0 ±0.5	1.3 ±0.5
Partitioning							
Atmospheric growth rate	1.7 ±0.1	2.8 ±0.1	3.4 ±0.1	3.1 ±0.1	4.0 ±0.1	4.5 ±0.1	6.3 ±0.2
Ocean sink	1. ±0.5	1.5 ±0.5	1.9 ±0.5	2.2 ±0.5	2.3 ±0.5	2.6 ±0.5	3.0 ±0.5
Residual terrestrial sink	1.7 ±0.7	1.7 ±0.8	1.6 ±0.8	2.6 ±0.8	2.6 ±0.8	3.1 ±0.8	1.9 ±0.9

Recent estimates (Ciais *et al.*, 2013; Landschützer *et al.*, 2014; Le Quéré *et al.*, 2016; Wanninkhof *et al.*, 2013) indicates that roughly one quarter of the anthropogenic CO_2 emitted in the last 20 years was taken up by the ocean, at a mean rate of about 1.4–2.6 Pg C yr^{-1}. In contrast, the coastal ocean has been largely ignored in global carbon budgeting due to the limited number of available local studies reports areas. These regions are the most biogeochemically active areas, it receives inputs of nutrient and organic matter from land and rivers, exchanges matter and energy with open ocean and atmosphere, and host strong biological activity (Borges *et al.*, 2005). Continental shelves are heterogeneous and the air-sea CO_2 flux shows latitudinal variations, as has been described by different authors (Borges *et al.*, 2005; Cai *et al.*, 2006; Chen *et al.*, 2013). At mid-high latitudes coastal oceans act as a sink while at low latitudes act as a source. Overall, marginal seas act as a sink but the budgets fall within the 0.18–0.45 Pg C yr^{-1} range (Borges *et al.*, 2005; Chen *et al.*, 2013; Laruelle *et al.*, 2014; Wanninkhof *et al.*, 2013). Those estimates are based on extrapolations from limited data sets, therefor quantifying the magnitude and variability of the coastal air-sea CO_2 exchange and carbon fluxes are required to better quantification of ocean uptake.

The main objective of this work is to improve our knowledge of the continental shelf role as a sink or source of CO_2 at a specific location, South African coastal sea, and assess whether there are any trends that could be related to interannual variability. The information discussed derived from QUIMA-VOS line *in situ* measurements (www.carboocean.org and www.carbochange.b.uib.no).

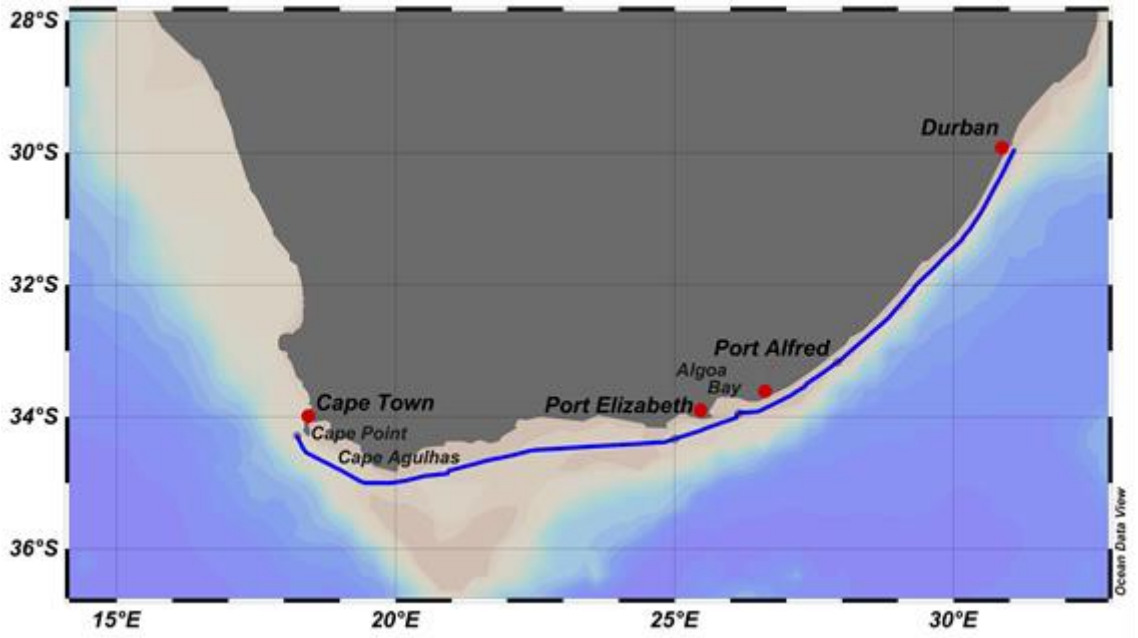

Figure 1. South Africa map. Red point indicate docking ports and blue line shows the vessel track.

1.2 South African Coastal Region

The near-coastal ocean off South Africa (Fig. 1) is a highly dynamic environment with a contrast between the shallow, well-stratified and relatively calm water over the Agulhas Bank, and the rapid, deep and turbulent flows of the Agulhas Current. This western boundary current influence in a complicated way most of this coastal region, it generates shelf-edge upwelling, creates border eddies, meanders and filaments of warm and salt water. Between Cape Point (-34°21'S-18°29'E) and Cape Agulhas (34º49'S-20º00'E) an intermittent wind-driven upwelling is formed but constitutes the southernmost upwelling cell of the Benguela system. East of Cape Agulhas the coastal morphology creates the required conditions to occur upwelling during easterly winds, especially at speeds higher than 6 ms^{-1}(Lutjeharms, 2006). From Cape Agulhas to Algoa Bay a well-developed continental shelf alters the behavior of Agulhas Current. Once the Agulhas water has passed Port Elizabeth the shear instabilities start to grow and the Ekman veering in the bottom boundary layer resulting in bring water onto the shelf. A well circumscribed upwelling cell take place during 80% of the time off Port Alfred (33º36'S-26º53'E) and the driving forces are both the wind parallel to the coast as the passing of a costal jet from

a narrow to a wider shelf (Lutjeharms *et al.*, 2000; Lutjeharms, 2006). The water that outcropped is South West Indian Central Water from 500 m depth, it is characterized by salinity around 35.2 and temperature less than 13 ºC. Due to water stratification and the strength of the upwelling, water outcropped is partially mixed with surface water and their temperature lies between 14 - 17ºC (Lutjeharms *et al.*, 2000). During summer and spring surface water shows minimum temperatures. The northern part of Agulhas current, from Algoa Bay to the border between South Africa and Mozambique, flows poleward along a narrow shelf where the current trajectory shows little variation. In this section water masses characteristic are South Indian Tropical Surface Water (temperature over 22 ºC) and South West Indian Subtropical Surface Water, with temperatures about 17.5 ºC (Lutjeharms *et al.*, 2000).

The monsoonal winds through the Mozambique Channel influence the Agulhas Current system with maximum transport during austral summer and minimum during austral winter (Lutjeharms, 2006). Furthermore, the passage of offshore meanders at the inshore edge generates path variations (Biastoch *et al.*, 1999; Lutjeharms *et al.*, 2000). This variability and the associated distribution of surface water temperature affect the regional climate. South Africa is regarded as semi-arid region and estuarine environments are characterized by small deltas (Laruelle *et al.*, 2010)

Unlike the west coast, where a few studies relating to the carbon dioxide have been carried out (Bakker *et al.*, 1999; González-Dávila *et al.*, 2009; Monteiro, 1996; Santana-Casiano *et al.*, 2009), the east and south coasts of South Africa are poorly examined. Over the continental shelf two locations had been studied (at 35º42'S− 20º6'E and 34º6'S−26º11'E) and indicated that the region acts as a sink of atmospheric CO_2, -2.41 mol C m^{-2} yr^{-1} and -4.03 mol C $m^{-2}yr^{-1}$ respectively (Chen *et al.*, 2013). It should be indicated that those studies only consider one (summer) and two (summer and autumn) seasons, respectively, and data should be considered as estimative. The mean annual net air-sea flux for CO_2 estimated by Takahashi *et al.* (2002), based on climatological distribution of surface water pCO_2 and NCEP/NCAR 41-year mean wind speed, shows a similar negative values (∼-2.0 mol C m^{-2} yr^{-1}). However, in more recent estimations (Takahashi *et al.*, 2009) the density flux is less negative (∼-1.5 mol C m^{-2} yr^{-1}). On the other hand, for the west region south of 32ºS the sink strength appears similar to that described above with values that range between -2 mol C m^{-2} yr^{-1} in August and -4 mol C m^{-2} yr^{-1} in November (Santana-Casiano *et al.*, 2009). Finally, South Africa is located in the temperate region and this area is commonly defined as a moderate sink of CO_2 (0 to -1 mol C m^{-2} yr^{-1}) (Laruelle *et al.*, 2014).

Despite the vast increase in the amount of data in last years, the spatial and temporal coverage for some regions are still quite poor. The continental shelf off South Africa is

one of these regions and its importance is not just local. The Agulhas system plays a key role in ocean circulation and climate, not only on the nearby coast. The leakage of warm and saline water from Indian to Atlantic Ocean through the Agulhas Current impacts the strength of the Atlantic Meridional Overturning Circulation (AMOC). This leakage is increasing under anthropogenic climate changes (Beal *et al.*, 2011). Also, the alteration of wind stress curl over South Indian Ocean could lead to an offshore movement of the Agulhas Current core position with possible consequences on rainfall pattern, ecology of estuaries and coastal ocean circulations (Lutjeharms & De Ruijter, 1996).

2. Material and methods

2.1 Temperature, salinity, and xCO_2measurements

From 2005 to 2012, except 2009 and 2010, four different container cargo ships (MSC-MARTINA, MSC-GINA, MSC-BENEDETTA, LARS MAERSK) were equipped with an automated underway xCO_2 system, developed by Craig Neill, to measure temperature, salinity and CO_2 molar fraction (xCO_2) in surface water and low atmosphere. These volunteer observing ships (VOS) were operating on a route from Northern Europe via Las Palmas (where the data were collected) to South Africa, docking at Cape Town (33º55'S-18º25'E), Port Elizabeth (33º57'S-25º36'E) and Durban (29º53'S-31º03'E).

Figure 2. Automated underway xCO_2 system. On the right side the *dry* box and on the left the *wet* box. No *deck* box or other components, like water pump and CO_2 gas cylinder, are shown.

The instrumental components (Fig. 2) were installed in two different place of the ship. The *wet* box, that contains all components of the flowing seawater system (equilibrator, condenser and water flow meter among others), and the *dry* box, that encloses the electronics components (the LICOR™ analyzer, computer and power supply) were placed in the engine room. In contrast the global positioning system (GPS), pressure sensor and air intake were located on the deck (*deck* box).

Water was drawn from the ship's uncontaminated seawater supply, at flows over 60 l min^{-1}, and passed through a plexiglass equilibrator (3 l min^{-1}), where the water CO_2 content is equilibrated with the gas present in the chamber. This gas forms a closed loop which circulates through the system and carrying the sample from the equilibrator to the analyzer (Li-Cor™ model 6262 infrared CO2/H2O detector), that evaluates seawater and atmospheric molar fraction of CO_2. Before that, this gas passes through a Peltier system and NAFION® tubes (Pierrot *et al.*, 2009) to remove water vapor prior to analysis (DOE, 1994). Every 3h the analyzer is calibrated with four different standard gases provided by the National Ocean and Atmospheric Administration (NOAA) and traceable to the World Meteorological Organization (WMO). The mixing ratios of standards are 0.0, 250 ppm, 380 ppm and 490 ppm of CO_2 in air. The precision of the system is superior to 0.5 µatm and the accuracy estimated with respect to the standard gases is 1 µatm.

To control de correct equipment operation, different types of sensors are used. Accurate measurement of temperature in the different system enclosures are important in order to determine fugacity of carbon dioxide (fCO_2), due to the isochemical dependence of fCO_2 on temperature is about 16 µatm $^oC^{-1}$. In the main water intake an SBE38 thermometer continuously monitored the surface seawater temperature (SST), while a SBE21 thermo-salinograph (TSG) was located close to the xCO_2 system, and annually calibrated (total estimated error of 0.01ºC and 0.005 in salinity). Another thermometer was also positioned in the equilibrator. The temperature differences between the seawater intake and the TSG depended on the equipment location and change in the different ships (0.23±0.05ºC on the MSC-MARTINA, 0.06±0.01ºC on the MSC-GINA and MSC-BENEDETTA, and 0.1±0.05ºC on the LARS MAERSK).

2.2 Determination of fugacity and fluxes of CO_2

The procedure to generate fCO_2 data from xCO_2 measurement consist in 3 step (DOE, 1994; Pierrot *et al.*, 2009): (1) calculate the equilibrator pCO_2 value (Eq. 1), by back-correcting the dry mole fraction to 100% humidity according to the saturated water vapor pressure (Eq. 2), pH_2O, at the equilibrator temperature; (2) estimate *in situ* pCO_2 (Eq. 3) applying a correction to account for the SST; and (3) obtain fCO_2 (Eq. 4) by correcting pCO_2 values with virial coefficient (Eq. 5 and Eq. 6). All equation used are shown in Table 2.

The exchange of CO_2 across the air-sea interface can be determined as the product of the difference between partial pressure of CO_2 in the surface water and in the overlying

air, the gas transfer velocity, k (ms^{-1}), and the aqueous-phase solubility of the gas, s (mol m^{-3} Pa^{-1}). The CO_2 flux (FCO_2) is usually expressed as (Eq. 7):

Table 2. Equations used to estimate fCO2 from xCO2 measurement (DOE, 1994; Pierrot *et al.*, 2009).

(1) pCO_2 in the equilibrator (100% humidity):

$$(pCO_2)_{T_E,wet} = xCO_2[P_{Eq} - pH_2O] \quad \text{(Eq. 1)}$$

Water vapor pressure:

$$pH_2O = \exp[24.4543 - 67.4509(100/T_E) - 4.8489\ln(T_E/100) - 0.000544\ S] \quad \text{(Eq. 2)}$$

(2) *pCO_2 at in situ conditions:*

$$(pCO_2)_{SST} = (pCO_2)_{T_E,wet} \cdot \exp[0.0423(SST - T_E)] \quad \text{(Eq. 3)}$$

(3) fCO_2 at in situ conditions:

$$(fCO_2)_{SST} = (pCO_2)_{SST} \cdot \exp\left[\frac{(B(CO_2)_{SST} + 2(1 - xCO_2)^2 \cdot \delta(CO_2)_{SST})P_{atm}}{R \cdot SST}\right] \quad \text{(Eq. 4)}$$

Virial coefficient of pure carbon dioxide gas (cm^3 mol^{-1}):

$$B(CO_2)_{SST} = -1636.75 + 12.0408\ SST - 3.27957 \times 10^{-2}SST^2 + 3.16528 \times 10^{-5}SST^3 \quad \text{(Eq. 5)}$$

Virial coefficient of carbon dioxide in air (cm^3 mol^{-1}):

$$\delta(CO_2)_{SST} = 57.7 - 0.118\ SST \quad \text{(Eq. 6)}$$

T_E: equilibrator temperature (K)	SST: sea surface temperature (K)
S: salinity	P_{atm}: atmospheric pressure (atm)
R: gas constant (82.0578 $cm^3 atm\ mol^{-1}\ K^{-1}$)	

$$FCO_2 = k \cdot s \cdot (pCO_{2,sw} - pCO_{2,atm}) = k \cdot s \cdot \Delta pCO_2 \quad \text{(Eq. 7)}$$

There are different settings for estimate the gas transfer velocity and it is often parameterized in terms of wind speed, although others factor (boundary layer stability, breaking waves, bubbles, and rain) must influence its variability (Wanninkhof *et al.*, 2009). This models assumes different transport mechanisms that are involved in the transfer and may lead to variations in FCO_2 of ~10% (Laruelle et al., 2014). In this study, CO_2 exchange coefficients were estimates using three parameterizations (Table 3) described by Wanninkhof (2014), KW'14 (Eq. 8), (Wanninkhof, 1992), KW'92 (Eq. 9), and Nightingale et al. (2000), KN'00 (Eq. 10). The choice of these parameterizations was based on the wind speed range and to allow comparisons with previous works, which usually used the quadratic relation proposed by Wanninkhof (1992). From 2005 to 2008 wind speed data were derived from SeaWinds sensor installed on the QuikScat satellite and provided by the CERSAT (http://cersat.ifremer.fr) with daily resolution and spatial

resolution of 1º×1º. On the other hand, between 2011 and 2012 wind speed records, also provided by the CERSAT, were derived from the ASCAT scatterometer onboard MetOp-A[2]. The spatial resolution is approximately 0.25º in longitude and latitude and the temporal resolution is 24 hours. All values were referenced to 10 m height. Do to the fact that wind speeds derived from scatterometers short-term expression of W'92 parameterization was taking into account.

Table 3. Gas transfer velocity (*k*) parameterizations based on wind speed velocity registered at 10m height (u_{10}^2) and normalized to a Schmidt number (*Sc*) computed for salinity and sea surface temperature.

Author	Equation	
Wanninkhof (1992)	$KW'92 = 0.31u_{10}^2(Sc/660)^{-1/2}$	(Eq. 8)
(Wanninkhof, 2014)	$KW'14 = 0.251u_{10}^2(Sc/660)^{-1/2}$	(Eq. 9)
Nightingale *et al.* (2000)	$KN'00 = [0.333u_{10} + 0.222u_{10}^2](Sc/660)^{-1/2}$	(Eq. 10)

2.3 Computational method

In order to eliminate erroneous values due to poor measurements, data were manually de-spiked and although when temperature or salinity are missing for less than ½ h these values can be interpolated from another temperature or salinity (Pierrot *et al.*, 2009), in this highly variable region this is not appropriate. Also, data recorded between Cape Town and Durban was averaged every 0.25º in longitude to obtain a better definition of transition zones and improve the upwelling cells description.

Since the seawater properties (SST, salinity and pCO_2) change with the time in response to the solar heating cycle, climatological and atmospheric variations, all measurements were fitted to a single reference year (2007) in order to compute any seasonality related to the solar heating cycle and local physical forcing. In this first step it is necessary to assume that between 2005 and 2012 pCO_2 concentrations have not changed. Every longitudinal 0.25º average data were fitted to a sinusoidal expression to obtain the climatological cycles of SST, salinity, wind and fCO_2 (atmospheric and oceanic). The wave function is given by (Eq. 11):

$$y = a + b(\sin 2\pi(x - 2005)) + c(\cos 2\pi(x - 2005)) + d(\sin 4\pi(x - 2005)) + e(\cos 4\pi(x - 2005)) + f(x - 2005) \quad \text{(Eq. 11)}$$

where *y* is the variable of interest, *x* is the date (year fraction) and the six terms (*a*, *b*, *c*, *d*, *e* and *f*) are unique for each province and parameter. The coefficient *a* defines the

average value, while coefficients *b*, *c*, *d* and *e*, define the harmonic function. Finally, term *f* represents the interannual variability. All coefficients are collected in the APPENDIX.

In a second step, by fixing all the harmonic terms the variables (SST, salinity, wind and fCO_2) were recalculated for the period 2005 and 2012 to compare the experimental and the observed results. Also, de FCO_2 was recalculated using the estimated values.

The normalization of the fCO_2 values to the average value of sea surface temperature (T_{mean}) in the three different regions allowed to remove the effects of the temperature on the observed fCO_2, following (Eq.12):

$$(fCO_2\ at\ T_{mean}) = fCO_2 \cdot \exp[0.0423(T_{mean} - SST)] \qquad \text{(Eq. 12)}$$

3. Results

3.1 Hydrographic situation

A west-to-east increase in surface temperature (Fig. 3) was observed in the twenty-eight voyages made over the QUIMA-VOS line between Cape Town and Durban. The track was divided in three regions (West, South and East) to calculate the mean temperature, presented in Table 4. Deviations from normal trend were detected at three well-defined locations: between 18º25'-20ºE, 26º-28ºE and at ~31ºE. The highest values were found over the East Region (Fig. 3 and Table 4), reaching 27 ºC during summer and 20 ºC in winter. Conversely, above the West Region lowest temperatures were detected and showed values that range between 22 ºC and 15 ºC during summer and winter, respectively. Surface temperatures under 15 ºC were observed on 53.3% of tracks around 19ºE.

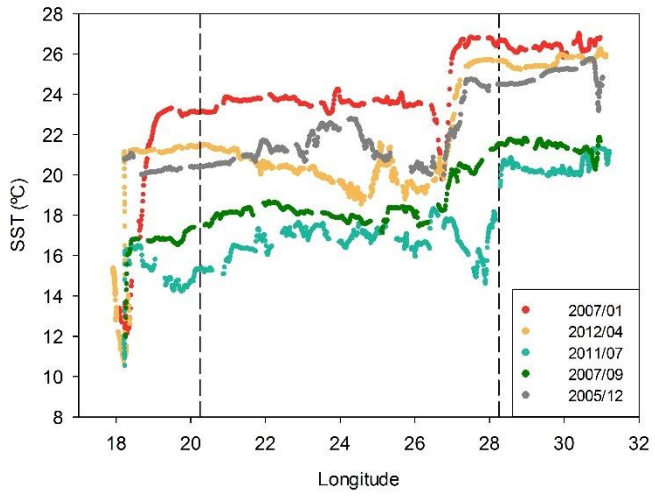

Figure 3. Sea surface temperature (ºC) along the VOS line for five selected cruises in order to show interannual variability. Dash line indicates the boundaries between the West and South Regions (20º15'E) and between South and East Regions (28º30'E).

The area enclosed by 26ºE and 28ºE represent a transition zone between the Agulhas Current and the Agulhas Bank conditions. Minimum records off Algoa Bay vary between 14 ºC and 17 ºC, but the eastern and western temperature gradients are different. On the west side were less pronounced, only 10% of the time a difference higher than 1ºC was measured with respect to the surrounding areas (23-25ºE). On the east side temperature vary in the range of 2 and 10 units during the most extreme episodes with respect to the east area. It is important to highlight that minimum temperatures were recorded more frequently on track closest to the coast (on journeys from Durban), however track difference are not clear. Also between Cape Point and Cape Agulhas low values were recorded (10-14 ºC) and the front showed gradients from 4.0 ºC up to 11 ºC.

Table 4. Mean sea surface temperature (ºC), seawater fugacity of CO_2 (µatm) and normalized fCO_{2sw} (µatm) to the averaged SST with respectively standard deviation (± SD) grouped by austral seasons and regions, defines as: West Region (18º15'E–20º15'E), South Region (>20º15'E–28º30'E) and East Region (>28º30'E). Note: winter estimates were based on only two journeys.

Parameter	Region	Winter	Spring	Summer	Autumn
SST	West	15.02 ± 1.26	16.75 ± 2.44	18.99 ± 3.37	17.57 ± 3.41
	South	17.71 ± 1.43	18.69 ± 2.42	21.163 ± 2.26	20.08 ± 2.37
	East	20.77 ± 0.54	22.75 ± 1.51	25.63 ± 1.41	25.04 ± 1.60
$fCO_{2,sw}$	West	337.96 ± 32.60	330.26 ± 33.91	316.77 ± 90.66	389.47 ± 67.24
	South	327.47 ± 27.31	325.70 ± 39.33	323.71 ± 60.40	351.03 ± 24.34
	East	344.57 ± 12.65	356.65 ± 18.59	371.27 ± 10.34	366.63 ± 13.25
$NfCO_{2,sw}$	West	374.47 ± 55.26	341.76 ± 66.86	303.85 ± 120.15	397.26 ± 129.11
	South	355.59 ± 37.65	340.39 ± 59.63	303.41 ± 67.23	346.45 ± 48.02
	East	392.09 ± 20.68	374.25 ± 39.07	344.35 ± 23.44	348.17 ± 19.40

Salinity presented an averaged value among seasons and years of 34.98 ±0.36. Recorded values range from 34.53 to 35.2, the last one were found near Port Alfred during summer and autumn, that also followed the lowest temperatures (13-17 ºC). Maxima were also found near Durban but none had temperatures below 24 ºC.

Along South African continental shelf winds ranging from 1.1 ms^{-1} to more than 15 ms^{-1}. Neither clear longitudinal variability nor seasonal changes were identified. Normally values around 8.09 ms^{-1} (± 2.86 ms^{-1}) were observed.

3.2 fCO_2 distribution and variability

Seawater fugacity of CO_2 ($fCO_{2,sw}$) distribution over the coastal region presented relatively constant values with maximum and minimum in well-defined locations. Excluding measurements made near Cape Point and Algoa Bay, the fugacity range between 300 µatm and 380 µatm. Some examples of this variability are presented in Fig. 4a, for the same cruises presented in Fig. 3. Table 4 includes mean values of $fCO_{2,sw}$ calculated by region and season.

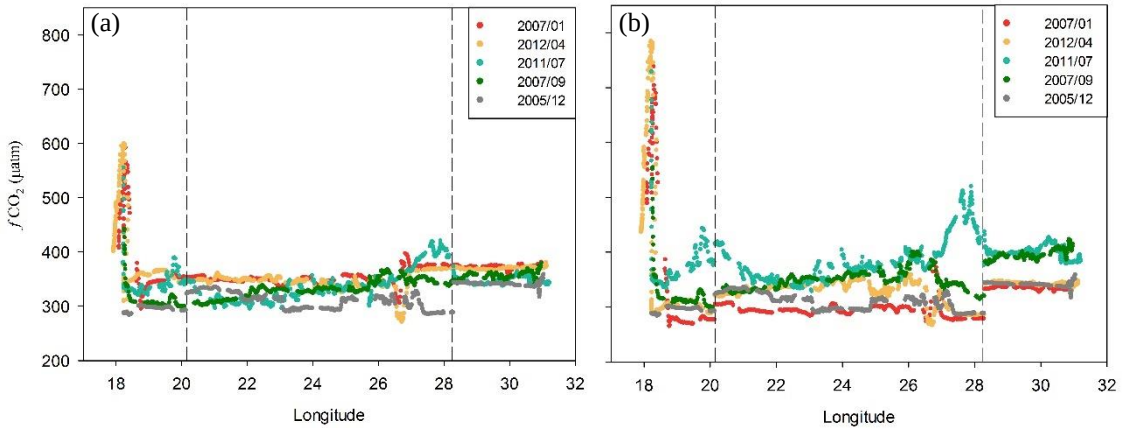

Figure 4. Longitudinal and interannual variability of sea water fCO_2values at *insitu* conditions (a) and at mean temperature (b) from five representative cruises along the QUIMA-VOS line. Dashed vertical lines indicates the boundaries between the West and South Regions (20º15'E) and between South and East Regions (28º30'E).

Around 18ºE in the West Region (18º15'E–20º15'E), the presence of cold water match in most of cases with high $fCO_{2,sw}$, although less frequently minimum values were also observed. It is a really variable area that not showed a clear seasonality as temperature is not the main controlling factor. Low fCO_2 records were measured during summer (~220 in February 2012) and early spring (~160 µatm in March 2007), while from June to November the fugacity showed values equal to or greater than those recorded between 19º and 20ºE. During March 2007 and May 2006 fugacities higher than 600 µatm were also recorded.

Between 20º15'E and 28º30'E (South Region, 20º30'E-28º30'E), $fCO_{2,sw}$ slightly rise following the increase in temperature. Deviation from the trend took place between 26ºE-28ºE, where the maxima differences in $fCO_{2,sw}$ (~215µatm) were measured in November 2012. Throughout the year, values higher than the rest of the South and East regions took place. Only during summer (February 2012 and November 2012) the values were lower than those measured in the West Region.

Easter of Algoa Bay (East Region, 28º45'E-31º15'E), fCO_2 exhibited higher and more uniform values (~361.3 µatm) compared to those in the southern area. Deviation from

this stability was detected on the northern part of the region, near Durban, where variations (± 17.5 µatm) were less pronounced than the Cape Town ones. Minimum records around 303 µatm were measured in September 2007, maximum values (~466.8 µatm and ~442.85 µatm) corresponds to September 2011 and July 2011. Both presented temperatures around 19ºC.

In order to remove thermodynamics effects on the fugacity variability, the $fCO_{2,sw}$ was normalized to a constant temperature for each region (Fig. 4b), using the same equation indicated in Table 2 in order to obtain the fCO_2 at *in situ* conditions. The figure shown more extreme values near 18ºE while minimums values close Durban are less pronounced. The greater fugacity gradient near Durban (~50µatm) was recorded on January 2005, coinciding with a SST gradient of ~3ºC. Out of these locations values are more similar.

Over the entire database the atmospheric fugacity of CO_2 ($fCO_{2,atm}$) showed a mean value of 373.82 ±10.2 µatm that ranged between 377.0 ± 4.4 µatm in summer and 371.8 ± 6.2 µatm in winter. On averaged, western region showed greater atmospheric CO_2 and from west to east a difference of ~2 µatm was observed.

3.3 CO_2 fluxes

Fluxes of CO_2 (FCO_2) were calculated using three parameterizations, as indicated in the methodology section, and included in Table 5 for the various regions, years and equations used. Differences between estimations over the same period and region were very low and differences match with a wide range of wind speeds. For example, fluxes estimated for the West region in 2007 (Table 5) corresponds with winds in the range of 5 and 15 ms^{-1}. On the other hand, values obtained for the same track were quite similar

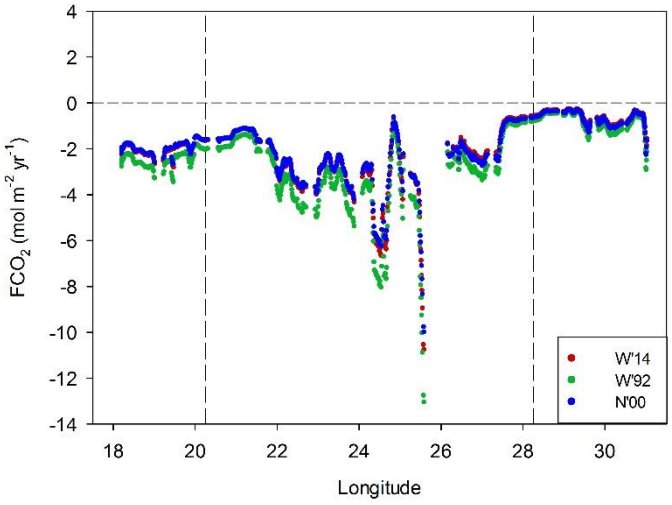

Figure 5. CO_2 fluxes (mol $m^{-2}yr^{-1}$) obtained with the three different parameterizations for December 2005 track. Vertical dashed lines indicate the boundaries between regions while horizontal dashed line highlight the zero flux value. Red points indicates FCO_2 estimated with Wanninkhof (2014), green ones obtained with Wanninkhof (1992) and blue dots were fluxes estimated with Nightingale *et al.* (2000).

although KW'92 values were higher than others. This is also observed in Fig. 5 that represent one example of fluxes estimated along one journey. Finally, in order to discuss the relationship between FCO_2 with others measurements and works, data computed from KW'92 were considered.

Table 5. Mean fluxes of CO_2 (mol m^{-2} yr^{-1}) following the Wanninkhof (1992) (KW'92), Wanninkhof (2014) (KW'14) and Nightingale *et al.* (2000) (KN'00) parameterizations. Values were computed over the three different regions and years using wind speed at 10 m height and observed data. Standard deviation (± SD) was also included.

Year	West			South			East		
	KW'92	KW'14	KN'00	KW'92	KW'14	KN'00	KW'92	KW'14	KN'00
2005	-2.9 ± 0.61	-2.35 ± 0.49	-2.27 ± 0.45	-2.19 ± 1.73	-1.76 ± 1.42	-1.75 ± 1.33	-0.61 ± 0.65	-0.45 ± 0.48	-0.48 ± 0.51
2006	-3.06 ± 4.49	-2.5 ± 3.79	-2.53 ± 3.67	-2.15 ± 4.77	-1.78 ± 4.02	-1.79 ± 3.79	-0.96 ± 1.7	-0.74 ± 1.34	-0.76 ± 1.31
2007	-4.47 ± 7.81	-3.72 ± 6.85	-3.42 ± 5.98	-2.05 ± 2.04	-1.67 ± 1.74	-1.64 ± 1.57	-0.82 ± 1.22	-0.65 ± 0.95	-0.65 ± 0.96
2008	-4.2 ± 3.51	-3.7 ± 3.19	-3.27 ± 2.73	-2.27 ± 1.77	-1.88 ± 1.5	-1.91 ± 1.45	0.23 ± 0.62	0.17 ± 0.47	0.18 ± 0.49
2011	-2.23 ± 1.96	-2.06 ± 1.85	-1.79 ± 1.57	-3.58 ± 3.34	-3.05 ± 2.85	-2.82 ± 2.51	-2.85 ± 2.12	-2.24 ± 1.69	-2.23 ± 1.58
2012	-0.19 ± 6.44	-0.08 ± 6.27	-0.19 ± 4.94	-1.65 ± 1.04	-1.35 ± 3.74	-1.37 ± 3.22	-0.08 ± 1.2	-0.04 ± 0.99	-0.07 ± 0.91

Positive fluxes indicate that the oceanic CO_2 content is higher than the atmospheric ones, acting the system as a source for this gas. Longitudinal variation match temperature and fugacity behavior, showing positive values in few records located near Cape Town, Port Alfred and Durban, also data collected during the same journey showed both positive and negative values.

From 18º15'E to 20º30'E, FCO_2 ranged between ~-32.23 and ~33.70 mol m^{-2} yr^{-1}. Maximum FCO_2 took place during April 2012 (33.70 mol m^{-2} yr^{-1}) and March 2007 (19.56 mol m^{-2} yr^{-1}). The lowest records also correspond with March 2007 (-32.23 mol m^{-2} yr^{-1}) and April 2012 (-14.68 mol m^{-2} yr^{-1}) and matched with mean wind speeds around 14.20 ms^{-1}, respectively. All fluxes higher than 18.25 mol m^{-2} yr^{-1} match with a wind speed that surpass 9.36 ms^{-1}. On the other hand, the highest speeds (~16.17 ms^{-1}) were recorded in October 2012 and correspond with a flux about 19.19 mol m^{-2} yr^{-1}. The averaged flux over the entire data set for this region showed a value of -2.16 ± 5.77 mol m^{-2} yr^{-1}.

As occurred along the West region, in the southern area maxima and minima fluxes took place during the same months: March 2006 (16.03 mol m^{-2} yr^{-1}, -20.67 mol m^{-2} yr^{-1}) and November 2012 (14.49 mol m^{-2} yr^{-1}, -15.45 mol m^{-2} yr^{-1}) that matched with winds higher than 13 ms^{-1}. From 21ºE to 26ºE fluxes were pretty constants. The averaged flux observed over this section was -2.32 ± 3.63 mol m^{-2} yr^{-1}.

At longitudes higher than 28º30'E, mean fluxes were around zero with maxima values about 13.80 and 7.95 mol m^{-2} yr^{-1} (March 2006 and November 2012) and minima around -9.55 mol m^{-2} yr^{-1} and -5.22 mol m^{-2} yr^{-1} (September 2011 and March 2007). The wind field along this region was quite stable and range between ~6 ms^{-1} and ~13 ms^{-1}. On average, the flux reached -1.01 ± 1.99 mol m^{-2} yr^{-1}.

The averaged fluxes estimated by region and year (Fig. 6) indicated the strength of uptake or release of carbon dioxide change along the time and that each area show a different behavior. For the period 2005 to 2012, negative values were determined in all years and regions (with the exception for the east section in 2008) acting the area as sink of CO_2 with an averaged value for the full area (18º15'E-31º15'E) of -1.88 ± 3.69 mol m^{-2} yr^{-1}.

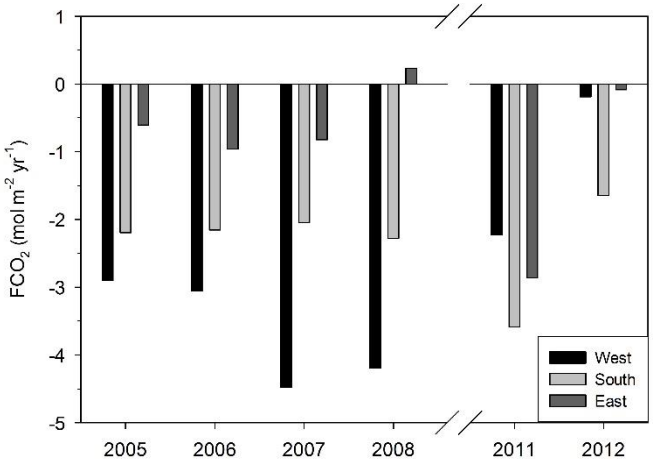

Figure 6. Mean fluxes of CO_2 (mol m^{-2} yr^{-1}) computed for each region and year following Wanninkhof (1992). Regions defines as: West Region (18º15'E–20º15E), South Region (>20º15'E–28º30E) and East Region (>28º30'E).

3.4 Fits of harmonic functions

The climatological seasonal cycles and interannual trends of sea surface temperature, seawater fugacity, atmospheric fugacity, wind and salinity were estimated over the single 0.25º in longitude. Fitted coefficient, collected in the APPENDIX, showed different behaviors depending on the longitudinal range over which the averages were calculated. Negative trends (coefficient *f* of APPENDIX tables) mean that the parameters tend to decrease over time while positive tendencies indicate that recent measurements are higher than previous ones. Both fugacities (atmospheric and oceanic), salinity and wind speed

presented negative trends along almost all the longitudes with wide range of R^2 (~0.1-0.8). On the other hand, temperature *f* term varies from -0.32 to 0.49 and showed more positive trends than other variables.

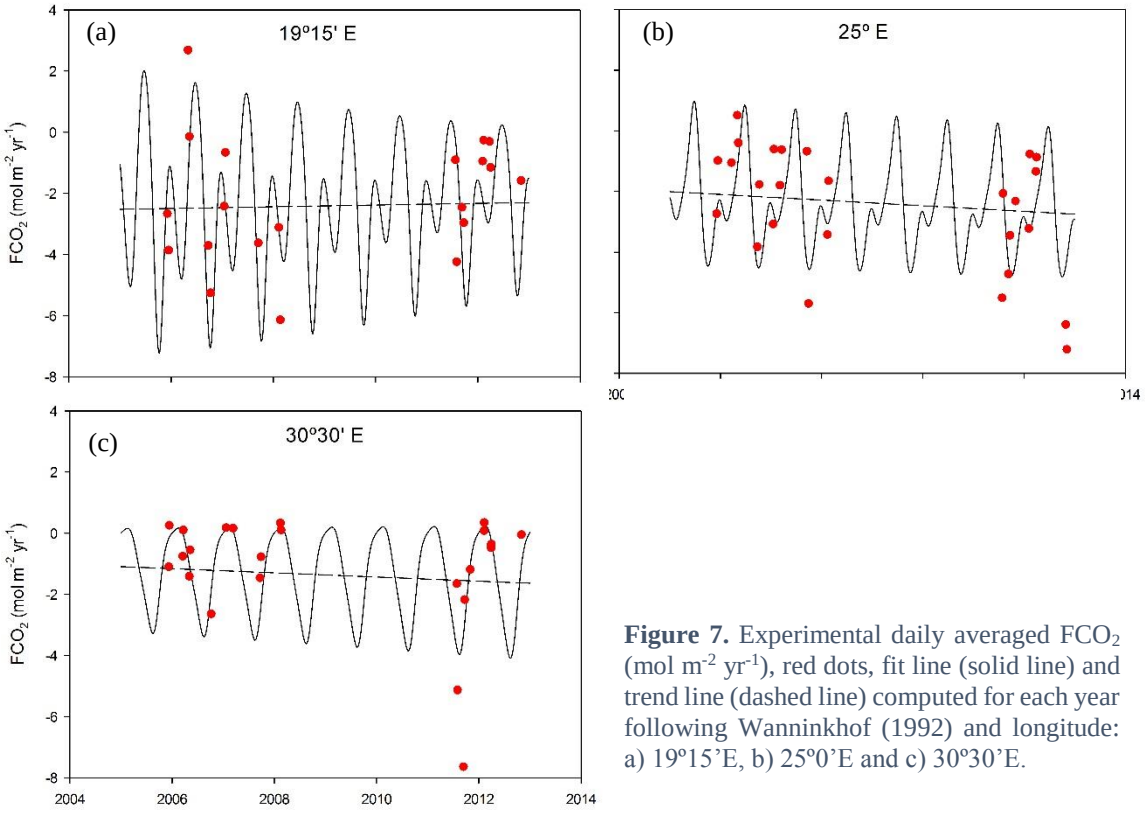

Figure 7. Experimental daily averaged FCO_2 (mol m^{-2} yr^{-1}), red dots, fit line (solid line) and trend line (dashed line) computed for each year following Wanninkhof (1992) and longitude: a) 19º15'E, b) 25º0'E and c) 30º30'E.

Fitting all these terms for the single variable a new FCO_2 was estimated for the period between January 2005 and December 2012, filling the gap with no data (2009-2010). Fig. 7 illustrate some examples of the interannual variability obtained at 19º15'E, 25ºE and 30º15'E. Total flux of CO_2 was obtained as the sum of the singular FCO_2 estimated over every longitude (Fig. 8a) to understand their role as a sink or source. Except at 18ºE and 28ºE where fluxes were positive for some years the rest of regions and years, uptake of CO_2 dominated over the areas. However, values obtained at 18º15'E, 28ºE and 31º15'E shows an inverse behavior from 2005 to 2010, increasing in some locations and decreasing in others, as represented in Fig. 8a.

Fig. 8b represents the mean fluxes estimated by region and year, different interannual variations were observed. The West Region exhibited a decrease in its capacity to uptake CO_2 of 0.061 ± 0.019 mol m^{-2} yr^{-1}, being more pronounced from 2008 to 2012 (0.131 ± 0.011 mol m^{-2} yr^{-1}). The South and East Regions became more sink over the years with speeds of 0.036 ± 0.001 mol m^{-2} yr^{-1} and 0.037 ± 0.002 mol $m^{-2}yr^{-1}$, respectively. These values could be compared with mean trends (*f* terms from APPENDIX tables) of variables used to estimate the FCO_2, computed over each region.

The seasonal difference of total FCO_2 by longitude (Fig 9) shows the effect of sea surface temperature especially over the East region (longitude > 28ºE). Also over the West and South region a seasonal difference can be observed, near 18ºE minimum values are higher during spring and summer and about 20-21ºE minimums take place during autumn and winter. Small release of gas from the surface ocean around Cape Town and Port Alfred with unique source episode at 20ºE during autumn.

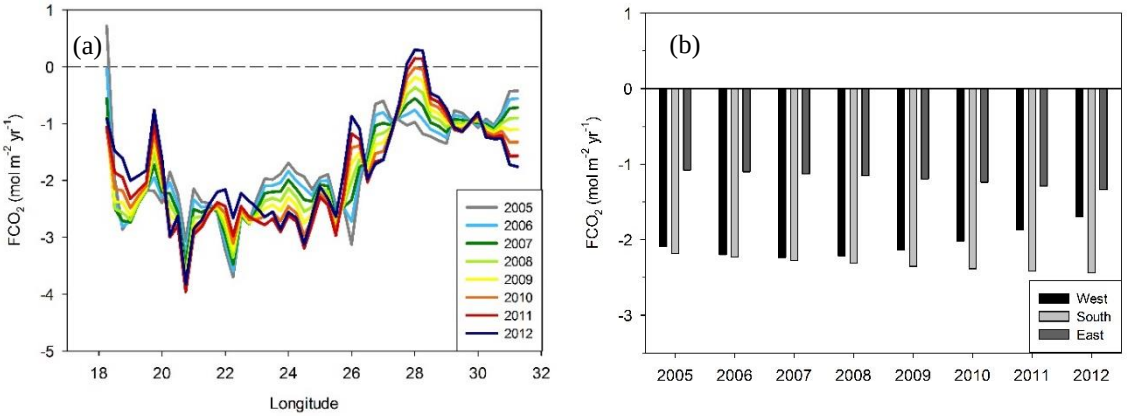

Figure 8. Total fluxes of CO2 (mol m^{-2} yr^{-1}) computed over each longitude and year represented as a west to east variation (a) and as mean value (b) in order to show the interannual variability of the coastal region.

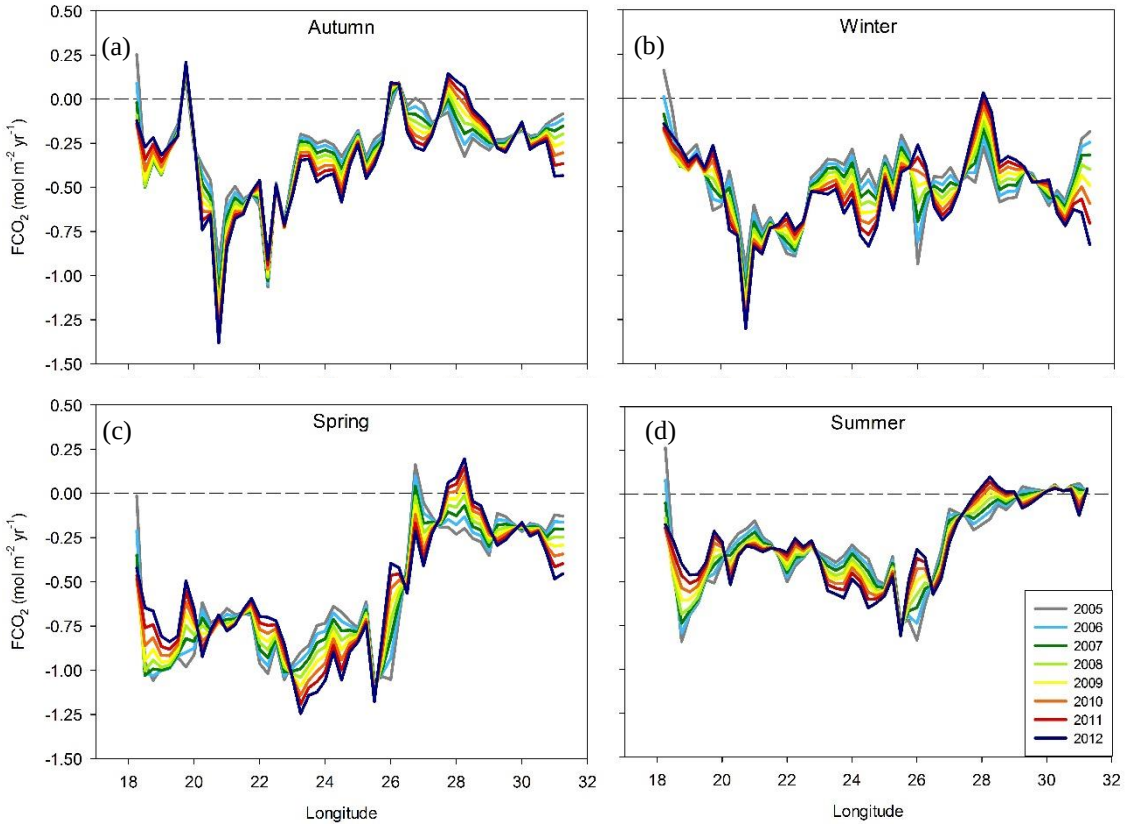

Figure 9. Seasonal variation of total flux (mol m^{-2} yr^{-1}) along each longitude and year estimated as the sum of fluxes obtained with the model fit. Dashed line represents the equilibrium between surface water and atmospheric exchange. a) Autumn, b) winter, c) spring and d) summer.

Finally, the mean FCO_2 obtained with harmonic fit output is -2.04 ± 1.65 mol m^{-2} yr^{-1}, similar to that indicated above the only experimental values were used. Regional averages were also calculated and showed the following values: West Region -2.06 ± 2.10 mol m^{-2} yr^{-1}, South Region -2.33 ± 1.58 mol m^{-2} yr^{-1} and East Region -1.19± 1.11 mol m^{-2} yr^{-1}. Considering that the vessel track covers 1490 km of coast line and assuming that data collected are uniform to a distance of 50 km at both side of the ship track (surface $1490 \cdot 10^8$ m^2), the South African coastal region is acting as a sink of 3.66 ± 0.10 Tg C yr^{-1} for the period 2005 to 2012 (1 Tg = 1 Mton = 10^{12} g), showing an interannual increase of 0.04 ± 0.006 Tg C yr^{-1}.

4. Discussion

4.1 Hydrographic situation

The temperature increased along longitude between Cape Town and Durban resulting from the contrast of relatively cold water over the Agulhas Bank and the warm Agulhas Current water (Lutjeharms, 2006). From west to east the first upwelling cell, located near Cape Town, was present through the seasons but the front temperature gradient were more important during summer, coinciding with the description given by Lutjeharms and Stockton (1991). This upwelling is controlled by winds, furthermore is subject to a complex coastal topography which alters the wind pattern and during summer the cell reaches its greatest development. As indicated by Lutjeharms *et al.* (2000) upwelled water occurs more than 40% of the time in accordance with result presented in this study. The change in temperature described for the northern front, the same cell in a previous study (González-Dávila *et al.*, 2009), showed lower values (4.5 ºC) than those obtained here (4-11 ºC), because the surface temperature of South Benguela system is lower than the one for the Agulhas Bank.

The second upwelling cell found off Algoa Bay, like the first, did not shown a clear seasonality but during summer the minimum in temperature is stronger. As described by different studies (Lutjeharms *et al.*, 2000; Lutjeharms & De Ruijter, 1996), winds parallel to the coast are more important during summer, however they are not the only driving force. This would explain the intermittent presence of minimum temperature. Furthermore, the passage of offshore meanders in the inshore edge of Agulhas Current explain the greater presence of upwelled water on journeys closest to the coast (Lutjeharms *et al.*, 2000). With respect to outcropped water, temperature and salinity characteristics corresponds to conditions of South West Indian Central Water that reaches the surface after mixing with surface and intermediate water (Lutjeharms *et al.*, 2000), producing changes in the temperature values especially in the 24-25ºE (Fig 3).

In the South Region, Lutjeharms (2006) found that winds from the west dominated during summer (February), specially over Agulhas Current. In October and November maximum average wind speed > 4 ms^{-1} were localized at Port Elizabeth, while the strong winter winds (>4.7 ms^{-1}) occur from May to August. In accordance with summer description, wind data presented in this work showed maximum values in October but not near Port Elizabeth.

4.2 *f*CO_2 variability

The distribution of CO_2 along the QUIMA-VOS line followed the same behavior of temperature. *f*CO_2 slightly increased form west to east and extreme values were recorded near Cape Town, Port Alfred and occasionally at Durban, also coinciding with maximum and minimum temperatures. This relationship confirms the upwelling presence in well-defined locations (Rouault *et al.*, 2010) that bring up, among other species, high rich CO_2 waters. Generally, outside these regions the remaining records showed surface values lower than atmospheric measurements, as reports by González-Dávila *et al.* (2009) for the South Benguela System.

Outcropped water with temperature lower than 17 ºC in summer or 14 ºC in winter coincided with salinity around 35 and fugacity higher than 400 µatm. These features correspond to the outcropped of South West Indian Central Water described in hydrographic investigations made over the continental shelf off South Africa (Lutjeharms *et al.*, 2000; Lutjeharms, 2006). Near Algoa Bay, the temperature minima were not as strong as near Cape Point. Strong mixing of waters off Port Alfred and the presence of a more developed upwelling in the first location (Lutjeharms *et al.*, 2000) resulted in the observed temperature difference. Low fugacity values after normalized to a constant temperature in the upwelling cells are explained by the photosynthetic uptake of CO_2 using the nutrient provided by the outcropped water. Moreover, nutrients coming from runoff particularly during summer and autumn (James *et al.*, 2013) could also favor the increase in productivity and reduce *f*CO_2 values.

Surface Agulhas Bank water presented temperatures about 18 ºC while Agulhas Current water showed 26.5 ºC (Lutjeharms *et al.*, 2000). The different origin on those water masses could explain the difference between the *f*CO_2 at *in situ* conditions (Fig. 4a) and at normalized temperature (Fig. 4b). As mentioned above the temperature strongly controls the solubility of gases (16 µatm/ºC for CO_2). The temperature effect was also detected on averaged data collected in Table 4. Higher fugacities match with greater temperatures (summer and East Region) except for the October mean, where the temperature was low and the fugacity was high. This was due to the presence of a well-

developed cell upwelling that injects rich CO_2 waters into the surface, not being consumed by the organisms or exported from the area.

4.3 FCO_2 over the coastal region

As shows in Table 5, the choice of different formulations for the gas transfer coefficient may lead to variations in FCO_2. The nature of this difference is related to the methodology applied to estimate the piston coefficient values and the dependence (linear, quadratic or cubic) established with the wind speed at 10 m height. Wanninkhof (1992), W'92, used the global bomb ^{14}C to fit a quadratic dependence of gas exchange on wind speed that should be applicable at steady winds (wind speeds derived from scatterometers or radiometers). Later, his work in 2014 (Wanninkhof, 2014), KW'14, improved the relationship using a revised global ocean ^{14}C inventory and improved wind speed products. The last one show a smaller uncertainty than W'92 due to "an improved understanding of the processes and a better quantification of global winds", as indicated by the author. This equation should provide good estimate at wind speed between 3 and 15 ms^{-1}, when physical and chemical processes in boundary layers do not impact on gas transfer. Finally, the polynomial equation proposed by Nightingale *et al.* (2000), KN'00, is based on small-scale dual-tracer studies and try to allows the impact of bubble on the transfer velocity. Each of these parameterizations fit better at one wind speed range than another and there are different studies that compare the existing parameterizations (Bender *et al.*, 2011; Goddijn-Murphy *et al.*, 2016). For example Wanninkhof (1992) overestimate the gas transfer velocity at winds higher than 5 ms^{-1}. Nightingale *et al.* (2000) and Wanninkhof (2014) show very similar values between 0 and 10 ms^{-1} but at higher velocities Nightingale results are lower than Wanninkhof estimations. Below 8 ms^{-1} KN'00 generates values slightly higher than KW'14. Differences indicated in Table 5 could be explained by this behavior and reveal why variations between FCO_2 estimated with diverse parameterizations were different along the track (Fig. 5).

As indicated previously, FCO_2 match with fCO_2 and wind variations so at locations where the wind is maximum and the surface water is undersaturated or oversaturated an accused peak was seen. On the other hand, oversaturated waters followed by minimum temperatures and salinities indicate the presence of outcropped water. If seawater pCO_2 is lower than atmospheric ones this is related to biological carbon dioxide uptake and/or the solubility pump. The study made by Shannon *et al.* (1984) highlight that the east coast of South Africa has different mesoscalar structures which develop well defined fronts and control the chlorophyll distribution. These processes explain the presence of maxima and minima FCO_2 along the same track, as specified for March 2006, March 2007, April 2012 and November 2012.

When we compare the FCO_2 estimated from the observations and those calculated with the harmonic functions can be seen that the differences are relatively small and, in the case of the fluxes recalculated with the fitting, the associated error is smaller. For this reason, hereinafter reference will be made to the FCO_2 calculated with the harmonic functions.

Fluxes obtained along the West region (-2.06 mol m^{-2} yr^{-1}) show similar values than those reported for the South Benguela system. Santana-Casiano *et al.* (2009) described fluxes that range between -2 and -4 mol m^{-2} yr^{-1} (28-34ºS) while González-Dávila *et al.* (2009) indicated values of 1.17 and -3.24 mol m^{-2} yr^{-1}, respectively for 2006 and 2007, for latitudes higher than 32ºS. In a more recent work of Gregor and Monteiro (2013) a net annual CO2 sink of -1.4 mol m^{-2} yr^{-1} was obtained. Differences could be related with the location that is not the same and the temporal resolution.

South area FCO_2 (-2.33 mol m^{-2} yr^{-1}) only can be compared with the values indicated by Chen *et al.* (2013) for two specific locations (20.1ºE,-35.7ºN and 26.2ºE,-34.1ºN) which annual flux were -2.41 and -4.03 mol m^{-2} yr^{-1}, respectively. For similar longitudes (20ºE and 26º15'E) the FCO_2 (Fig. 8a) obtained by fitting harmonic terms, showed averaged values of -2.18 and -1.76 mol m^{-2} yr^{-1}. For same locations Chen *et al.* (2013) also indicated some seasonal values: 20.1ºE,-35.7ºN presented summer and autumn FCO_2 of -5.79 mmol m^{-2} d^{-1} and -7.42 mmol m^{-2} d^{-1} (in this study -4.58 mmol m^{-2} d^{-1} and -3.17 mmol m^{-2} d^{-1}, respectively); while 26.2ºE,-34.1ºN showed a summer flux of -11.04 mmol m^{-2} d^{-1} (compared with -6.84 mmol $m^{-2}d^{-1}$ obtained here). The latitudinal difference is higher between points around 20ºE than near 26ºE however the flux discrepancy is reverse (closest points are more different). Other factors like temporal resolution or changes in surface conditions could explain this variation. Over the Agulhas Bank hydrographic conditions are more stable than ones observed off Algoa Bay (~26ºE) where clearly circumscribed upwelling cell is centered (Lutjeharms *et al.*, 2000).

East region showed lower values (-1.19 mol $m^{-2}yr^{-1}$) than the others areas reported and the mean FCO_2 is more in line with the value obtained by Laruelle *et al.* (2014), -0.54 mol $m^{-2}yr^{-1}$, than the previous indicated by (Chen *et al.*, 2013), -4.03 mol $m^{-2}yr^{-1}$. Both of them are described for the Agulhas Current system.

Overall, the flux estimates per year and region (Fig. 8b) indicated that on averaged the coastal region was undersaturated and act as a sink of CO_2, following the path of sea surface temperature, wind field and difference between the atmospheric and seawater content of carbon dioxide. From this figure, it seems that the flux over the years varied more in the western region while in the South and East regions it remained practically stable. A decreased in the sequestration capacity in the westernmost section was seen.

However, it should be considerate the difference in temporal coverage data from one region to another. Also, based on mean values recorded in Table 5, most years and regions can be both a source and sink.

The averaged CO_2 sink recorded over the South African coastal region, -2.04 mol m^{-2} yr^{-1}, agreed well with values reported in other studies. The mean annual net flux estimated by Takahashi *et al.* (2002) for 1995 reach values around -2 mol m^{-2} yr^{-1}. In the subsequent estimation of flows (Takahashi *et al.*, 2009), the magnitude decreases to ∼-1.50 mol m^{-2} yr^{-1} (in both cases values have been derived from a graph). Also, the result shown in this study is consistent with the idea that high and mid-latitude coastal regions act as a sink of CO_2 (Borges *et al.*, 2005; Cai *et al.*, 2006; Chen *et al.*, 2013).

4.4 Seasonal and interannual trends

Throughout the year, as indicated in Tables A1, A2, A3, A4 and A5 parameters records increase or decrease following different slopes. From 2005 to 2012, the sea surface temperature increase with a relatively higher drop around 18º15'E and 26ºE while negative values were only found along the transition zones (Table A1). Opposite to it, others parameters showed negative trends. The decrease in wind speed could explain the sea surface temperature increases but the variation of $fCO_{2,sw}$ can be affected by other factors. The comparison of mean FCO_2 variation along the regions (Fig 8b) exposed that the West Region losing the ability to capture CO_2 over time. To discern the wind effect on fluxes the averaged FCO_2 were also calculated using a mean wind speed (8.17 ms^{-1}) and, for the region between 18º15'E and 20º15'E, the FCO2 showed an increasing intake so this area behavior was controlled by wind speed changes. In the southern region, there was a slight increase in sink capacity and a decrease in wind speed. However, the FCO_2 obtained with a constant wind showed positive values, so the variability in this zone can be considered as controlled by both the changes in the physical-chemical conditions and by the atmospheric dynamics. On the other hand, in the East Region the CO_2 flux obtained at 8 ms^{-1} not presented variations, which indicates that the wind is the main factor controlling gas exchange at these longitudes and since the decrease of the wind was very low it continued acting as a sink.

As described by Rouault *et al.* (2010), negative SST trends off Algoa Bay are due to an increase in upwelling favorable winds (south-easterly and easterly), with a cooling of 0.4ºC per decade. Also, for Agulhas Current an increasing in temperature was defined (0.7 ºC per decade). Both of them are relate to an intensification of trade winds in the South Indian Ocean, as result of the expansion and intensification of the Hadley Cell in the Southern Hemisphere (Lu *et al.*, 2007). These variations could increase the rainfall

for the east coast while a decrease along the west coast and adjacent interior. This lead to a hydrological cycle variation with important consequences for rivers, estuaries and coastal ocean. In addition to this variation in Hadley Cell, (Bakun, 1990) proposed that under global warming the different temperatures between the land and the nearby ocean could enhance the pressure gradient and generate upwelling-favorable winds. On the other hand, salinity (Table D), presented negative values along all longitudes with very weak slopes not following the temperature trend. This is because the surface temperature is more affected by solar radiation and wind than by upwelling.

The FCO_2 obtained by fitting the harmonic functions and recorded in Fig. 7 shows a very weak tendency to increase with time. These graphs indicate that more positive values take place during late summer and spring while negative values match with austral winter moths in response to temperature effect. Also in Fig. 9 the temperature effect over gas solubility is indicated by the enhancement of positive FCO_2 during summer along all longitudes but especially over the East region (>28º15'E). As it is indicated in Fig. 8a and Fig. 9. 18º15'E correspond with the upwelling cell near Cape Town that decrease in FCO_2, 28ºE indicate the transition zone between the Agulhas Current condition and the Agulhas Bunk conditions where FCO_2 increase along time and finally 31º15'E. This seems to indicate the reinforcement on upwelling especially near Durban. As described by Lutjeharms and De Ruijter (1996) both increase and decrease in wind stress curl over South Indian Ocean could be translate into a higher occurrence frequency for Natal Pulse (meanders initiated off the Natal coast and move downstream as a soliton) that alters the seawater fugacities.

From 2005 to 2012 averaged FCO_2 increased from -3.47 to -3.75 Mton yr^{-1} and the averaged value over all years and regions was -3.66 Mton yr^{-1}. Compared with values obtained at South Benguela, -1.7 and -2.0 Mton yr-1 (Gregor & Monteiro, 2013) or 2.8 Mtons yr-1 (Monteiro, 2010) is higher but could be explained by the difference years and data length considered.

5. Conclusion

The coastal ocean off South Africa represents a very dynamic region were upwelling, filament, eddies and water from Agulhas Current controls the distribution of fCO_2, salinity and temperature. The journey from Cape Town to Durban was divided in three sectors. The West region (from Cape Town to 19.25ºE) is characterized by minimum temperatures (~10-14%) and maximum fugacities (> 600µatm). Surface characteristics increased to east due to the mixing with Agulhas Current water. The South Region is characterized by transition waters between the cold Agulhas Bank water and the warn Agulhas Current water. Near Port Alfred another upwelling cell take place, however minimums and maximum were less pronounced due to the mixing of upwelled and surface water. Also near Durban minimum values take place. This minimum of temperature and variable fCO_2 (minimum or maximum) not exhibited a clear seasonality.

Fluxes above the region were negative with important deviations. West region exhibited an averaged flux of -2.06 ± 2.10 mol m^{-2} yr^{-1}. Maximum values were estimated for the South Region (-2.33 ± 1.58 mol m^{-2} yr^{-1}) while minimum fluxes characterized the East sector (-1.19 ± 1.11 mol m^{-2} yr^{-1}). The averaged flux estimated over the entire region was -2.04 ± 1.65 mol m^{-2} yr^{-1}.

Throughout the year SST exhibited positive trends with different slopes, depending on the region. Interannual trends were different. fCO_{2sw}, fCO_{2atm}, wind, salinity and FCO_2 presented negative tendencies while SST showed positive slopes. Nevertheless, the tendencies were smooth and standard errors could reverse the trends. FCO_2 obtained from fitted variables showed a value of -3.66 ± 0.10 Tg C yr^{-1} and from 2005 to 2012 the South African Coastal Region uptake increased with a trend of 0.04 ± 0.006 Tg C yr^{-1}.

It is important to highlight that given the high variability of coastal regions always they require increasingly large records to understand and describe the behavior of the area. Especially when you want to discern any effect of climate change on these waters. More studies are needed to clearly distinguish any interannual trend over decadal changes affected by climate change.

Acknowledgments

The *Universidad de Las Palmas de Gran Canaria* is acknowledged for giving me the opportunity to perform this work. Thanks goes also to the Marine Science Faculty for supporting students in their education curriculum and to the QUIMA research group for take me in their team and giving me the opportunity to gain experience in this research work.

I would like to thank my supervisors, Dr. Melchor González Dávila and Dr. J. Magdalena Santana Casiano, for sharing their knowledge and guiding me through the process of developing this study.

References

Bakker, D.C., de Baar, H.J., de Jong, E., 1999. The dependence on temperature and salinity of dissolved inorganic carbon in East Atlantic surface waters. *Marine Chemistry*, 65, 263-280.

Bakun, A., 1990. Global climate change and intensification of coastal ocean upwelling. *Science*, 247, 198-201.

Bates, N.R., Astor, Y.M., Church, M.J., Currie, K., Dore, J.E., González-Dávila, M., Lorenzoni, L., Muller-Karger, F., Olafsson, J., Santana-Casiano, J.M., 2014. A time-series view of changing ocean chemistry due to ocean uptake of anthropogenic CO_2 and ocean acidification. *Oceanography*, 27, 126-141.

Beal, L.M., De Ruijter, W.P.M., Biastoch, A., Zahn, R., 2011. On the role of the Agulhas system in ocean circulation and climate. *Nature*, 472, 429-436.

Bender, M.L., Kinter, S., Cassar, N., Wanninkhof, R., 2011. Evaluating gas transfer velocity parameterizations using upper ocean radon distributions. *Journal of Geophysical Research Oceans*, 116.

Biastoch, A., Reason, C., Lutjeharms, J., Boebel, O., 1999. The importance of flow in the Mozambique Channel to seasonality in the greater Agulhas Current system. *Geophysical Research Letters*, 26, 3321-3324.

Borges, A., Delille, B., Frankignoulle, M., 2005. Budgeting sinks and sources of CO_2 in the coastal ocean: Diversity of ecosystems counts. *Geophysical Research Letters*, 32.

Cai, W.J., Dai, M., Wang, Y., 2006. Air-sea exchange of carbon dioxide in ocean margins: A province-based synthesis. *Geophysical Research Letters*, 33.

Chen, C.-T., Huang, T.-H., Chen, Y.-C., Bai, Y., He, X., Kang, Y., 2013. Air–sea exchanges of CO_2 in the world's coastal seas. *Biogeosciences*, 10, 6509-6544.

Ciais, P., Sabine, C., G. Bala, G., Bopp, L., Brovkin, V., Canadell, J., Chhabra, A., DeFries, R., Galloway, J., Heimann, M., Jones, C., Le Quéré, C., Myneni, R.B., Piao, S., Thornton, P., 2013. Carbon and Other Biogeochemical Cycles. In T.F. Stocker, D. Qin, G.K. Plattner, M. Tignor, S.K. Allen, J. Boschung, A. Nauels, Y. Xia, V. Bex, P.M. Midgley (Eds.), Climate Change 2013: The Physical Science Basis. Contribution of Working Group I to the Fifth Assessment Report of the Intergovernmental Panel on Climate Change. Cambridge, United Kingdom and New York, NY, USA., Cambridge University Press, 465-570.

DOE, 1994. Handbook of methods for the analysis of the various parameters of the carbon dioxide system in sea water. Washington, DC, ORNL/CDIAC-74.

Doney, S.C., Fabry, V.J., Feely, R.A., Kleypas, J.A., 2009. Ocean acidification: the other CO_2 problem. *Annual Review of Marine Science*, 1, 169–192.

Fuss, S., Canadell, J.G., Peters, G.P., Tavoni, M., Andrew, R.M., Ciais, P., Jackson, R.B., Jones, C.D., Kraxner, F., Nakicenovic, N., Le Quéré, C., Raupach, M.R., Sharifi, A.,

Smith, P., Yamagata, Y., 2014. Betting on negative emissions. *Nature Climate Change*, 4, 850-853.

Goddijn-Murphy, L., Woolf, D.K., Callaghan, A.H., Nightingale, P.D., Shutler, J.D., 2016. A reconciliation of empirical and mechanistic models of the air-sea gas transfer velocity. *Journal of Geophysical Research Oceans*, 121, 818–835.

González-Dávila, M., Santana-Casiano, J.M., Ucha, I.R., 2009. Seasonal variability of *f*CO_2 in the Angola-Benguela region. *Progress in Oceanography*, 83, 124-133.

Gregor, L., Monteiro, P., 2013. Is the southern Benguela a significant regional sink of CO2? *South African Journal of Science*, 109, 01-05.

Gruber, N., Gloor, M., Mikaloff Fletcher, S.E., Doney, S.C., Dutkiewicz, S., Follows, M.J., Gerber, M., Jacobson, A.R., Joos, F., Lindsay, K., Menemenlis, D., Mouchet, A., Müller, S.A., Sarmiento, J.L., Takahashi, T., 2009. Oceanic sources, sinks, and transport of atmospheric CO2. *Global Biogeochemical Cycles*, 23, 1-21.

Herr, D., Galland, G.R., 2009. People, the ocean and climate change. The ocean and climate change: tools and guidelines for action. Gland, Switzerland, IUCN, 72.

IPCC, 2014. Climate change 2014: synthesis Report. Contribution of working groups I, II and III to the fifth assessment report of the intergovernmental panel on climate change. Geneva, Switzerland, IPCC.

Jackson, R.B., Canadell, J.G., Le Quéré, C., Andrew, R.M., Korsbakken, J.I., Peters, G.P., Nakicenovic, N., 2015. Reaching peak emissions. *Nature Climate Change*, 6, 7-10.

James, N.C., van Niekerk, L., Whitfield, A.K., Potts, W.M., Götz, A., Paterson, A.W., 2013. Effects of climate change on South African estuaries and associated fish species. *Climate research*, 57, 233-248.

Landschützer, P., Gruber, N., Bakker, D., Schuster, U., 2014. Recent variability of the global ocean carbon sink. *Global Biogeochemical Cycles*, 28, 927-949.

Laruelle, G.G., Dürr, H.H., Slomp, C.P., Borges, A.V., 2010. Evaluation of sinks and sources of CO_2 in the global coastal ocean using a spatially-explicit typology of estuaries and continental shelves. *Geophysical Research Letters*, 37.

Laruelle, G.G., Lauerwald, R., Pfeil, B., Regnier, P., 2014. Regionalized global budget of the CO_2 exchange at the air-water interface in continental shelf seas. *Global Biogeochemical Cycles*, 28, 1199-1214.

Le Quéré, C., Andres, R.J., Boden, T., Conway, T., Houghton, R.A., House, J.I., Marland, G., Peters, G.P., van der Werf, G.R., Ahlström, A., Andrew, R.M., Bopp, L., Canadell, J.G., Ciais, P., Doney, S.C., Enright, C., Friedlingstein, P., Huntingford, C., Jain, A.K., Jourdain, C., Kato, E., Keeling, R.F., Klein Goldewijk, K., Levis, S., Levy, P., Lomas, M., Poulter, B., Raupach, M.R., Schwinger, J., Sitch, S., Stocker, B.D., Viovy, N., Zaehle, S., Zeng, N., 2013. The global carbon budget 1959–2011. *Earth System Science Data*, 5, 165-185.

Le Quéré, C., Andrew, R.M., Canadell, J.G., Sitch, S., Korsbakken, J.I., Peters, G.P., Manning, A.C., Boden, T.A., Tans, P.P., Houghton, R.A., Keeling, R.F., Alin, S., Andrews, O.D., Anthoni, P., Barbero, L., Bopp, L., Chevallier, F., Chini, L.P., Ciais, P., Currie, K., Delire, C., Doney, S.C., Friedlingstein, P., Gkritzalis, T., Harris, I., Hauck, J., Haverd, V., Hoppema, M., Klein Goldewijk, K., Jain, A.K., Kato, E., Körtzinger, A., Landschützer, P., Lefèvre, N., Lenton, A., Lienert, S., Lombardozzi, D., Melton, J.R., Metzl, N., Millero, F., Monteiro, P.M.S., Munro, D.R., Nabel, J.E.M.S., Nakaoka, S.I., O'Brien, K., Olsen, A., Omar, A.M., Ono, T., Pierrot, D., Poulter, B., Rödenbeck, C., Salisbury, J., Schuster, U., Schwinger, J., Séférian, R., Skjelvan, I., Stocker, B.D., Sutton, A.J., Takahashi, T., Tian, H., Tilbrook, B., van der Laan-Luijkx, I.T., van der Werf, G.R., Viovy, N., Walker, A.P., Wiltshire, A.J., Zaehle, S., 2016. Global Carbon Budget 2016. *Earth System Science Data*, 8, 605-649.

Le Quéré, C., Moriarty, R., Andrew, R.M., Canadell, J.G., Sitch, S., Korsbakken, J.I., Friedlingstein, P., Peters, G.P., Andres, R.J., Boden, T.A., Houghton, R.A., House, J.I., Keeling, R.F., Tans, P., Arneth, A., Bakker, D.C.E., Barbero, L., Bopp, L., Chang, J., Chevallier, F., Chini, L.P., Ciais, P., Fader, M., Feely, R.A., Gkritzalis, T., Harris, I., Hauck, J., Ilyina, T., Jain, A.K., Kato, E., Kitidis, V., Klein Goldewijk, K., Koven, C., Landschützer, P., Lauvset, S.K., Lefèvre, N., Lenton, A., Lima, I.D., Metzl, N., Millero, F., Munro, D.R., Murata, A., Nabel, J.E.M.S., Nakaoka, S., Nojiri, Y., O'Brien, K., Olsen, A., Ono, T., Pérez, F.F., Pfeil, B., Pierrot, D., Poulter, B., Rehder, G., Rödenbeck, C., Saito, S., Schuster, U., Schwinger, J., Séférian, R., Steinhoff, T., Stocker, B.D., Sutton, A.J., Takahashi, T., Tilbrook, B., van der Laan-Luijkx, I.T., van der Werf, G.R., van Heuven, S., Vandemark, D., Viovy, N., Wiltshire, A., Zaehle, S., Zeng, N., 2015a. Global Carbon Budget 2015. *Earth System Science Data*, 7, 349-396.

Le Quéré, C., Moriarty, R., Andrew, R.M., Peters, G.P., Ciais, P., Friedlingstein, P., Jones, S.D., Sitch, S., Tans, P., Arneth, A., Boden, T.A., Bopp, L., Bozec, Y., Canadell, J.G., Chini, L.P., Chevallier, F.C., Cosca, C.E., Harris, I., Hoppema, M., Houghton, R.A., House, J.I., Jain, A.K., Johannessen , T., Kato, E., Keeling, R.F., Kitidis, V.K., Klein Goldewijk, K.K., Koven, C., Landa , C.S., Landschützer, P., Lenton, A., Lima, I.D., Marland, G., Mathis, J.T., Metzl, N., Nojiri, Y., Olsen, A., Ono, T., Peng, S., Peters, W., Pfeil, B., Poulter, B., Raupach, M.R., Regnier, P., Rödenbeck, C., Saito, S., Salisbury, J.E., Schuster, U., Schwinger, J., Séférian, R., Segschneider, J., Steinhoff, T., Stocker, B.D., Sutton, A.J., Takahashi, T., Tilbrook, B., Van der Werf, G.R., Viovy, N., Wang, Y.-P., Wanninkhof, R., Wiltshire, A., Zeng, N., 2015b. Global carbon budget 2014. *Earth System Science Data*, 7, 47-85.

Lu, J., Vecchi, G.A., Reichler, T., 2007. Expansion of the Hadley Cell under global warming. *Geophysical Research Letters*, 34.

Lutjeharms, J., Cooper, J., Roberts, M., 2000. Upwelling at the inshore edge of the Agulhas Current. *Continental Shelf Research*, 20, 737-761.

Lutjeharms, J., De Ruijter, W., 1996. The influence of the Agulhas Current on the adjacent coastal ocean: possible impacts of climate change. *Journal of Marine Systems*, 7, 321-336.

Lutjeharms, J., Stockton, P., 1991. Aspects of the upwelling regime between Cape Point and Cape Agulhas, South Africa. *South African Journal of Marine Science*, 10, 91-102.

Lutjeharms, J.R.E., 2006. The Agulhas Current, Springer.

McKinley, G.A., Pilcher, D.J., Fay, A.R., Lindsay, K., Long, M.C., Lovenduski, N.S., 2016. Timescales for detection of trends in the ocean carbon sink. *Nature*, 530, 469-472.

Monteiro, P.M.S., 1996. The oceanography, the biogeochemistry and the fluxes of carbon dioxide in the Benguela upwelling system. University of Cape Town, South Africa, 354.

Monteiro, P.M.S., 2010. Eastern Boundary Current Systems. In K.-K. Liu, L. Atkinson, R. Quiñones, L. Talaue-McManus (Eds.), Carbon and nutrient fluxes in continental margins: a global synthesis, Springer Science & Business Media, 25-120.

Nightingale, P.D., Malin, G., Law, C.S., Watson, A.J., Liss, P.S., Liddicoat, M.I., Boutin, J., Upstill-Goddard, R.C., 2000. In situ evaluation of air-sea gas exchange parameterizations using novel conservative and volatile tracers. *Global Biogeochemical Cycles*, 14, 373-387.

Orr, J.C., Fabry, V.J., Aumont, O., Bopp, L., Doney, S.C., Feely, R.A., Gnanadesikan, A., Gruber, N., Ishida, A., Joos, F., 2005. Anthropogenic ocean acidification over the twenty-first century and its impact on calcifying organisms. *Nature*, 437, 681-686.

Pierrot, D., Neill, C., Sullivan, K., Castle, R., Wanninkhof, R., Lüger, H., Johannessen, T., Olsen, A., Feely, R.A., Cosca, C.E., 2009. Recommendations for autonomous underway pCO_2 measuring systems and data-reduction routines. *Deep Sea Research II*, 56, 512-522.

Rouault, M., Pohl, B., Penven, P., 2010. Coastal oceanic climate change and variability from 1982 to 2009 around South Africa. *African Journal of Marine Science*, 32, 237-246.

Sabine, C.L., Feely, R.A., Gruber, N., Key, R.M., Lee, K., Bullister, J.L., Wanninkhof, R., Wong, C., Wallace, D.W., Tilbrook, B., Millero, F.J., Peng, T.-H., Kozyr, A., Ono, T., Rios, A.F., 2004. The oceanic sink for anthropogenic CO_2. *Science*, 305, 367-371.

Santana-Casiano, J.M., González-Dávila, M., Ucha, I.R., 2009. Carbon dioxide fluxes in the Benguela upwelling system during winter and spring: A comparison between 2005 and 2006. *Deep Sea Research II*, 56, 533-541.

Shannon, L.V., Hutchings, L., Bailey, G.W., Shelton, P.A., 1984. Spatial and temporal distribution of chlorophyll in southern African waters as deduced from ship and satellite measurements and their implications for pelagic fisheries. *South African Journal of Marine Science*, 2, 109-130.

Sitch, S., Friedlingstein, P., Gruber, N., Jones, S., Murray-Tortarolo, G., Ahlström, A., Doney, S.C., Graven, H., Heinze, C., Huntingford, C., Levis, S., Levy, P.E., Lomas, M., Poulter, B., Viovy, N., Zaehle, S., Zeng, N., Arneth, A., Bonan, G., Bopp, L., Canadell, J.G., Chevallier, F., Ciais, P., Ellis, E., Gloor, M., Peylin, P., Piao, S.L., Le Quéré, C., Smith, B., Zhu, Z., Myneni, R., 2015. Recent trends and drivers of regional sources and sinks of carbon dioxide. *Biogeosciences*, 12, 653-679.

Takahashi, T., Sutherland, S.C., Sweeney, C., Poisson, A., Metzl, N., Tilbrook, B., Bates, N., Wanninkhof, R., Feely, R.A., Sabine, C., 2002. Global sea–air CO 2 flux based on

climatological surface ocean pCO 2, and seasonal biological and temperature effects. *Deep Sea Research II*, 49, 1601-1622.

Takahashi, T., Sutherland, S.C., Wanninkhof, R., Sweeney, C., Feely, R.A., Chipman, D.W., Hales, B., Friederich, G., Chavez, F., Sabine, C., Watson, A.J., Bakker, D.C.E., Schuster, U., Metzl, N., Yoshikawa-Inoue, H., Ishii, M., Midorikawa, T., Nojiri, Y., Körtzinger, A., Steinhoff, T., Hoppema, M., Olafsson, J., Arnarson, T.S., Tilbrook, B., Johannessen, T., Olsen, A., Bellerby, R., Wong, C.S., Delille, B., Bates, N.R., de Baar, H.J.W., 2009. Climatological mean and decadal change in surface ocean pCO_2, and net sea–air CO_2 flux over the global oceans. *Deep Sea Research II*, 56, 554-577.

Wanninkhof, R., 1992. Relationship between wind speed and gas exchange over the ocean. *Journal of Geophysical Research: Oceans*, 97, 7373-7382.

Wanninkhof, R., 2014. Relationship between wind speed and gas exchange over the ocean revisited. *Limnology and Oceanography*, 12, 351-362.

Wanninkhof, R., Asher, W.E., Ho, D.T., Sweeney, C., McGillis, W.R., 2009. Advances in quantifying air-sea gas exchange and environmental forcing. *Annual Review of Marine Science*, 1, 213-244.

Wanninkhof, R., Park, G.-H., Takahashi, T., Sweeney, C., Feely, R.A., Nojiri, Y., Gruber, N., Doney, S.C., McKinley, G.A., Lenton, A., Le Quéré, C., Heinze, C., Schwinger, J., Graven, H., Khatiwala, S., 2013. Global ocean carbon uptake: magnitude, variability and trends. *Biogeosciences*, 10, 1983–2000.

APPENDIX

Table A1. Seasonal fitting coefficients for SST (ºC) in 0.15º resolution and for the three regions, West (18º15'E−20º15'E), South (>20º15'E−28º30'E) and East (>28º30'E). Listing longitude (ºE), the coefficients (a, b, c, d, e and f), the standard error (ºC) of estimate and coefficient of determination (R^2).

Lon	a	b	c	d	e	f	St. error	R^2	Lon	a	b	c	d	e	f	St. error	R^2
18º15'	14.48	1.05	0.88	-0.73	0.35	0.49	3.09	0.12	25º15'	18.88	1.14	1.45	0.28	0.55	0.17	1.42	0.55
18º30'	16.48	1.21	1.50	-0.90	-0.56	0.22	2.65	0.20	25º30'	18.52	0.80	1.65	0.58	0.01	0.11	1.34	0.53
18º45'	17.26	1.28	1.95	-0.21	0.14	0.07	2.01	0.42	25º45'	18.26	0.89	1.17	0.99	-0.26	0.13	1.51	0.49
19º0'	17.52	1.04	2.12	-0.40	0.28	-0.01	1.99	0.41	26º0'	17.61	1.34	1.12	0.38	-0.11	0.37	2.16	0.34
19º15'	17.53	0.88	2.51	0.01	0.40	-0.09	1.93	0.49	26º15'	17.61	0.92	1.98	1.05	-0.23	0.34	2.25	0.39
19º30'	17.49	1.13	2.19	-0.29	0.22	-0.03	2.18	0.38	26º30'	18.49	1.13	0.04	0.24	0.84	0.38	2.81	0.14
19º45'	17.73	0.75	2.58	-0.07	0.56	-0.15	2.50	0.36	26º45'	18.66	1.49	-0.64	-0.20	1.25	0.44	3.21	0.15
20º0'	18.47	1.53	2.81	0.09	0.37	-0.14	2.09	0.55	27º0'	20.20	1.12	0.04	-0.12	1.59	0.12	3.37	0.14
20º15'	18.56	2.25	2.84	0.33	0.05	-0.03	0.58	0.96	27º15'	21.27	1.09	0.49	0.21	1.48	-0.13	3.38	0.17
20º30'	18.81	2.06	2.85	0.43	-0.06	-0.10	0.59	0.95	27º30'	21.78	0.81	1.52	-0.02	1.35	-0.25	3.35	0.18
20º45'	18.91	1.94	2.65	0.43	0.02	-0.10	0.68	0.93	27º45'	21.93	1.02	1.78	0.03	1.19	-0.27	3.38	0.22
21º0'	19.09	1.86	2.65	0.57	0.22	-0.14	0.79	0.91	28º0'	22.21	0.65	2.15	0.03	1.25	-0.32	2.80	0.30
21º15'	18.91	1.72	2.51	0.39	0.24	-0.10	0.96	0.86	28º15'	22.71	0.88	1.92	0.13	1.40	-0.27	2.23	0.44
21º30'	18.78	1.56	2.32	0.46	0.14	-0.03	0.98	0.82	28º30'	22.65	0.81	1.92	0.63	0.76	-0.08	2.25	0.38
21º45'	18.53	1.54	2.23	0.41	0.13	0.03	1.16	0.76	28º45'	22.58	1.50	1.78	0.39	-0.07	0.11	1.39	0.63
22º0'	18.34	1.42	1.95	0.33	0.17	0.08	1.44	0.62	29º0'	22.81	1.68	2.07	0.23	-0.23	0.14	1.06	0.77
22º15'	18.46	1.24	1.53	0.47	0.28	0.10	1.64	0.51	29º15'	22.72	2.03	2.08	0.01	-0.10	0.22	1.12	0.78
22º30'	18.53	1.10	1.77	0.96	0.19	0.08	1.56	0.57	29º30'	22.76	1.90	1.92	-0.05	-0.07	0.19	1.22	0.71
22º45'	18.56	1.04	1.73	1.48	0.28	0.09	1.44	0.67	29º45'	23.00	1.82	1.80	0.02	-0.04	0.14	0.95	0.80
23º0'	18.48	1.03	1.95	1.26	0.35	0.08	1.40	0.69	30º0'	23.04	1.88	2.08	0.18	-0.29	0.12	0.90	0.84
23º15'	18.63	1.15	1.92	0.83	0.38	0.08	1.50	0.61	30º15'	23.38	2.08	1.67	-0.34	-0.16	0.09	1.02	0.78
23º30'	18.63	0.96	1.70	0.51	0.52	0.17	1.53	0.53	30º30'	23.70	2.09	1.97	-0.06	0.00	0.06	0.58	0.93
23º45'	18.76	1.05	1.79	0.55	0.58	0.14	1.18	0.69	30º45'	23.72	2.76	1.62	-0.47	-0.29	0.24	1.84	0.67
24º0'	18.51	1.10	1.81	0.36	0.30	0.21	1.30	0.60	31º0'	23.55	2.22	1.70	0.04	0.08	0.04	0.59	0.94
24º15'	18.37	0.93	1.67	0.44	0.35	0.22	1.58	0.47	31º15'	23.65	2.03	1.81	0.00	-0.02	-0.08	0.49	0.97
24º30'	18.55	0.90	1.30	0.40	0.71	0.20	1.51	0.48									
24º45'	18.60	0.82	1.67	0.33	0.52	0.14	1.36	0.54									
25º0'	18.54	1.01	1.67	0.60	0.16	0.16	1.22	0.63									

Table A2. Seasonal fitting coefficients for fCO_{2sw} (µatm) in 0.15º resolution and for the three regions, West (18º15'E–20º15'E), South (>20º15'E–28º30'E) and East (>28º30'E). Listing longitude (ºE), the coefficients (a, b, c, d and e), the standard error (µatm) and coefficient of determination (R^2).

Lon	a	b	c	d	e	f	St. error	R^2
18º15'	397.72	2.56	-10.99	-4.78	19.08	-9.37	81.31	0.03
18º30'	368.77	-5.34	-20.48	-3.51	46.54	-9.40	74.10	0.14
18º45'	345.43	-5.41	-27.66	-18.30	38.04	-4.15	50.91	0.24
19º0'	345.20	-7.30	-22.78	-12.95	38.54	-5.25	51.43	0.22
19º15'	347.03	-1.44	-26.36	-14.75	35.95	-3.92	51.62	0.19
19º30'	344.74	6.99	-20.05	-15.47	25.53	-2.81	56.30	0.10
19º45'	342.39	24.55	-22.75	-19.39	13.55	1.71	69.33	0.08
20º0'	338.20	13.57	-11.28	-7.91	21.38	-0.65	56.70	0.08
20º15'	339.64	5.19	-6.99	-7.58	27.52	-3.74	52.46	0.11
20º30'	341.29	8.04	0.40	-5.64	26.66	-5.18	50.44	0.14
20º45'	340.45	7.70	1.74	-3.20	27.40	-4.58	49.67	0.15
21º0'	339.81	7.90	4.36	-2.38	26.45	-5.21	52.75	0.13
21º15'	334.63	11.17	1.36	-6.54	21.64	-3.37	49.57	0.12
21º30'	333.31	7.40	-1.22	-2.76	20.54	-2.86	50.73	0.08
21º45'	328.63	6.06	-3.70	-9.12	21.06	-2.14	51.37	0.08
22º0'	319.39	5.36	-9.29	-11.46	18.70	-1.16	50.37	0.06
22º15'	323.50	3.94	-9.96	-1.24	20.47	-2.13	55.26	0.05
22º30'	330.65	7.06	-9.32	-5.32	13.70	-2.41	52.91	0.03
22º45'	330.49	7.32	-12.45	11.18	17.82	-4.04	54.59	0.08
23º0'	336.16	2.44	-11.32	-0.95	18.32	-4.23	52.71	0.05
23º15'	336.45	2.25	-15.18	-5.91	18.28	-2.83	51.98	0.05
23º30'	332.82	-0.87	-15.76	-6.67	22.53	-1.63	49.09	0.07
23º45'	337.02	-0.97	-14.63	-8.54	24.39	-2.40	48.26	0.09
24º0'	341.16	-3.45	-14.29	-1.80	27.10	-3.09	45.38	0.12
24º15'	340.41	-2.26	-7.14	-3.77	22.04	-3.28	48.02	0.08
24º30'	337.91	-6.34	-9.90	1.40	18.95	-3.93	49.00	0.06
24º45'	334.07	-1.10	-15.01	-7.37	17.98	-2.87	50.02	0.06
25º0'	337.27	-0.21	-22.25	-8.82	25.56	-2.35	52.94	0.10
25º15'	336.65	0.01	-22.71	-10.53	23.13	-2.58	51.18	0.09
25º30'	335.92	-2.76	-31.73	-8.74	27.92	-3.46	54.04	0.12
25º45'	335.15	0.51	-34.32	-13.54	22.50	-3.66	58.66	0.12
26º0'	330.51	8.89	-36.32	-22.71	8.96	1.74	35.80	0.31
26º15'	343.79	9.37	-37.79	-25.88	5.88	-0.54	36.94	0.32
26º30'	349.33	-1.43	-21.39	-21.78	-4.84	-2.94	47.84	0.18
26º45'	363.90	-8.31	2.14	-22.60	-16.46	-4.74	46.64	0.20
27º0'	364.97	1.74	7.13	-3.44	-18.92	-4.34	43.65	0.08
27º15'	359.56	1.47	8.64	-2.58	-13.92	-1.75	50.44	0.03
27º30'	360.85	2.51	2.31	-4.20	-3.78	-0.41	50.02	0.01
27º45'	357.56	3.53	-0.34	-6.00	-9.96	1.77	45.95	0.03
28º0'	356.88	-0.31	-1.57	3.22	-10.91	2.30	32.32	0.06
28º15'	352.60	1.31	9.44	1.19	-14.87	2.87	31.95	0.07
28º30'	352.64	8.01	16.46	-2.26	-12.28	0.97	20.48	0.24
28º45'	351.38	4.58	15.97	-1.08	-8.95	0.69	16.24	0.24
29º0'	350.86	6.04	17.34	2.69	-5.93	0.11	9.39	0.57
29º15'	361.49	2.06	18.81	4.40	-10.80	-3.11	12.09	0.41
29º30'	359.25	2.53	17.89	4.54	-11.96	-2.16	10.56	0.46
29º45'	355.27	9.31	16.29	0.96	-4.13	-0.24	9.88	0.59
30º0'	357.10	8.27	15.01	-0.20	-3.63	-0.56	11.64	0.44
30º15'	359.60	7.58	15.69	1.06	-2.90	-0.88	13.75	0.37
30º30'	357.36	7.44	14.41	0.23	-3.04	-0.66	8.67	0.59
30º45'	358.78	8.32	13.62	2.49	1.66	-1.22	8.98	0.65
31º0'	365.82	4.58	8.12	6.13	-6.88	-2.53	14.72	0.27
31º15'	356.09	7.62	13.11	6.72	-11.45	0.14	6.86	0.83

Table A3. Seasonal fitting coefficients for $fCO_{2\ atm}$ (µatm) in 0.15º resolution and for the three regions, West (18º15'E–20º15'E), South (>20º15'E–28º30'E) and East (>28º30'E). Listing longitude (ºE), the coefficients (a, b, c, d and e), the standard error (µatm) and coefficient of determination (R^2).

Lon	a	b	c	d	e	f	St. error	R^2	Lon	a	b	c	d	e	f	St. error	R^2
18º15'	377.14	-2.36	-0.84	0.69	-2.50	-0.75	6.86	0.15	25º15'	377.49	-3.84	-1.58	0.60	-2.18	-1.18	6.53	0.24
18º30'	376.75	-2.28	-0.59	0.45	-2.95	-0.84	6.25	0.19	25º30'	375.87	-3.40	0.19	0.64	-3.80	-0.81	6.82	0.19
18º45'	374.20	-1.97	-0.75	0.37	-2.62	-0.15	6.38	0.16	25º45'	375.60	-3.07	-0.50	2.62	-2.98	-1.15	6.64	0.19
19º0'	373.69	-1.71	-0.44	0.14	-3.63	-0.09	6.80	0.18	26º0'	379.72	-4.87	0.84	1.66	-4.08	-1.78	7.09	0.26
19º15'	373.88	-1.70	-0.77	0.46	-3.80	-0.19	6.92	0.19	26º15'	373.58	-2.90	-1.04	2.60	-3.24	-0.68	6.29	0.21
19º30'	374.28	-2.29	-0.98	0.10	-2.91	-0.29	6.70	0.19	26º30'	373.13	-2.71	-1.69	2.71	-3.27	-0.57	6.47	0.21
19º45'	373.89	-1.83	-0.58	0.34	-3.14	-0.12	6.63	0.17	26º45'	372.61	-2.25	-1.81	2.52	-4.06	-0.34	6.26	0.27
20º0'	374.98	-3.52	-1.36	0.07	-3.05	-0.64	6.51	0.27	27º0'	374.34	-2.87	-0.84	2.70	-3.17	-0.84	6.35	0.19
20º15'	373.97	-2.93	-1.53	-0.28	-2.56	-0.26	6.37	0.25	27º15'	372.41	-2.15	-1.97	2.38	-3.81	-0.36	5.35	0.32
20º30'	374.74	-2.86	-2.44	-0.16	-1.98	-0.28	6.44	0.25	27º30'	372.77	-2.69	-2.60	2.98	-3.16	-0.44	5.46	0.32
20º45'	373.66	-2.66	-1.50	-0.31	-3.15	-0.22	6.41	0.27	27º45'	373.09	-3.30	-3.01	3.44	-2.24	-0.60	5.73	0.30
21º0'	374.44	-2.97	-0.97	-0.36	-2.58	-0.47	6.38	0.24	28º0'	372.62	-2.45	-2.17	2.64	-3.64	-0.34	5.81	0.28
21º15'	374.51	-3.01	-0.88	-0.15	-2.63	-0.49	6.44	0.23	28º15'	374.51	-3.13	-3.72	4.06	-2.07	-1.04	5.76	0.32
21º30'	374.60	-2.98	-0.78	0.05	-2.67	-0.54	6.42	0.22	28º30'	373.47	-3.88	-4.01	2.95	-2.29	-0.64	5.12	0.41
21º45'	374.20	-2.80	-1.31	-0.47	-2.79	-0.31	6.67	0.23	28º45'	373.57	-3.38	-5.21	3.04	-1.63	-0.59	5.07	0.43
22º0'	374.62	-2.96	-0.15	0.19	-2.90	-0.62	6.56	0.20	29º0'	373.02	-3.37	-3.47	3.60	-1.91	-0.62	5.43	0.36
22º15'	374.27	-2.57	-0.29	-0.31	-3.24	-0.42	6.24	0.22	29º15'	374.52	-3.27	-7.01	2.37	0.03	-0.45	5.59	0.39
22º30'	374.65	-3.18	0.44	-0.88	-2.98	-0.63	6.16	0.27	29º30'	375.59	-3.08	-7.68	2.23	0.73	-0.70	5.55	0.44
22º45'	375.01	-3.48	0.36	-0.61	-3.24	-0.61	6.78	0.26	29º45'	375.38	-3.50	-7.37	2.48	1.20	-0.79	6.03	0.45
23º0'	375.43	-3.02	-0.47	0.31	-3.31	-0.93	6.20	0.24	30º0'	374.26	-3.41	-5.78	3.20	-0.96	-0.63	5.17	0.42
23º15'	374.51	-3.40	-0.22	0.98	-3.36	-0.65	6.08	0.26	30º15'	378.78	-0.32	-5.36	0.63	-0.10	-0.18	3.87	0.46
23º30'	375.31	-2.75	-0.24	0.24	-3.00	-0.89	6.36	0.21	30º30'	375.44	-2.27	-7.67	1.65	0.49	-0.50	5.84	0.41
23º45'	374.32	-3.18	0.12	0.06	-3.45	-0.55	6.15	0.27	30º45'	377.49	-3.84	-1.58	0.60	-2.18	-1.18	6.53	0.24
24º0'	374.93	-3.06	-0.03	0.43	-3.09	-0.65	6.39	0.21	31º0'	375.87	-3.40	0.19	0.64	-3.80	-0.81	6.82	0.19
24º15'	374.88	-2.72	0.26	0.47	-3.55	-0.61	6.60	0.19	31º15'	375.60	-3.07	-0.50	2.62	-2.98	-1.15	6.64	0.19
24º30'	375.20	-2.68	-0.41	0.61	-3.18	-0.55	6.53	0.18									
24º45'	375.17	-3.27	0.36	1.27	-3.01	-0.81	6.42	0.18									
25º0'	375.05	-2.89	0.35	0.23	-3.31	-0.55	6.76	0.19									

Table A4. Seasonal fitting coefficients for salinity in 0.15º resolution and for the three regions, West (18º15'E−20º15'E), South (>20º15'E−28º30'E) and East (>28º30'E). Listing longitude (ºE), the coefficients (a, b, c, d and e), the standard error and coefficient of determination (R^2).

Lon	a	b	c	d	e	f	St. error	R^2	Long	a	b	c	d	e	f	St. error	R^2
18º15'	34.87	0.00	0.26	-0.07	0.08	-0.04	0.30	0.29	25º15'	35.20	-0.60	0.26	0.12	0.66	-0.19	1.92	0.12
18º30'	35.01	0.04	0.31	-0.16	-0.02	-0.04	0.30	0.32	25º30'	35.41	-1.12	0.24	0.09	1.45	-0.30	3.80	0.12
18º45'	34.96	0.02	0.37	-0.11	-0.07	-0.02	0.26	0.39	25º45'	35.48	-0.88	0.13	-0.50	1.77	-0.22	4.33	0.10
19º0'	34.94	0.04	0.35	-0.16	-0.13	-0.02	0.30	0.32	26º0'	35.33	-1.48	0.36	0.04	1.85	-0.36	4.61	0.16
19º15'	34.95	0.00	0.39	-0.12	-0.09	-0.04	0.24	0.44	26º15'	35.21	-1.02	0.32	0.09	1.11	-0.30	3.81	0.10
19º30'	34.98	0.04	0.38	-0.14	-0.05	-0.03	0.24	0.48	26º30'	35.32	-0.73	0.01	-0.01	1.22	-0.23	3.81	0.08
19º45'	34.96	-0.03	0.41	-0.12	-0.05	-0.04	0.25	0.44	26º45'	35.40	-1.02	0.11	0.13	1.28	-0.32	4.03	0.10
20º0'	34.98	0.05	0.39	-0.14	-0.08	-0.03	0.27	0.38	27º0'	35.24	-1.02	0.07	0.24	1.32	-0.28	3.87	0.10
20º15'	35.04	0.08	0.39	-0.11	-0.06	-0.04	0.27	0.42	27º15'	35.27	-1.01	0.07	0.23	1.32	-0.29	3.91	0.10
20º30'	35.05	0.07	0.40	-0.10	-0.05	-0.04	0.26	0.43	27º30'	35.32	-1.00	0.11	0.24	1.31	-0.31	3.96	0.10
20º45'	35.10	0.06	0.33	-0.09	0.00	-0.04	0.26	0.33	27º45'	34.94	0.09	0.28	0.10	0.02	-0.04	0.27	0.39
21º0'	35.06	0.04	0.41	-0.07	-0.02	-0.05	0.27	0.42	28º0'	34.97	0.06	0.25	0.08	0.09	-0.05	0.29	0.32
21º15'	35.02	0.01	0.39	-0.10	0.01	-0.05	0.26	0.43	28º15'	34.91	0.09	0.26	0.08	0.02	-0.04	0.28	0.33
21º30'	35.01	0.00	0.35	-0.09	0.00	-0.04	0.25	0.39	28º30'	34.94	0.08	0.26	0.07	0.02	-0.04	0.30	0.29
21º45'	34.98	-0.01	0.35	-0.07	0.00	-0.04	0.24	0.39	28º45'	34.95	0.11	0.24	0.08	0.04	-0.05	0.30	0.31
22º0'	34.96	-0.02	0.29	-0.09	0.01	-0.03	0.22	0.37	29º0'	34.93	0.12	0.26	0.10	0.03	-0.04	0.29	0.38
22º15'	34.96	-0.02	0.30	-0.05	0.01	-0.04	0.26	0.29	29º15'	35.00	0.13	0.24	0.08	0.02	-0.06	0.30	0.32
22º30'	34.95	0.00	0.31	0.00	-0.02	-0.03	0.29	0.23	29º30'	34.96	0.08	0.28	0.03	0.00	-0.04	0.32	0.23
22º45'	34.98	-0.02	0.33	0.03	0.02	-0.05	0.28	0.31	29º45'	34.95	0.09	0.28	0.09	0.04	-0.05	0.31	0.32
23º0'	34.99	-0.04	0.33	0.03	0.02	-0.05	0.30	0.29	30º0'	34.95	0.10	0.30	0.10	0.04	-0.05	0.31	0.36
23º15'	35.04	-0.03	0.30	-0.01	0.04	-0.07	0.30	0.26	30º15'	34.94	0.12	0.25	0.07	0.04	-0.03	0.33	0.26
23º30'	34.98	-0.07	0.33	0.02	0.06	-0.05	0.30	0.31	30º30'	35.00	0.07	0.29	0.04	0.03	-0.06	0.33	0.26
23º45'	34.98	-0.10	0.35	0.00	0.04	-0.05	0.34	0.27	30º45'	35.28	-2.10	1.06	0.96	1.59	-0.60	5.68	0.13
24º0'	34.99	-0.11	0.36	0.02	0.08	-0.05	0.34	0.32	31º0'	34.95	0.06	0.36	0.08	0.00	-0.05	0.33	0.33
24º15'	34.95	-0.07	0.29	0.03	0.10	-0.05	0.33	0.26	31º15'	34.92	0.30	0.42	0.01	-0.12	-0.01	0.32	0.67
24º30'	34.98	-0.08	0.25	0.04	0.14	-0.06	0.39	0.22									
24º45'	35.00	-0.10	0.25	0.03	0.16	-0.06	0.41	0.22									
25º0'	35.02	-0.10	0.27	-0.01	0.14	-0.07	0.45	0.20									

Table A5. Seasonal fitting coefficients for wind (ms^{-1}) in 0.15º resolution and for the three regions, West (18º15'E–20º15'E), South (>20º15'E–28º30'E) and East (>28º30'E). Listing longitude (ºE), the coefficients (a, b, c, d and e), the standard error (ms^{-1}) and coefficient of determination (R^2).

Lon	a	b	c	d	e	f	St. error	R^2	Long	a	b	c	d	e	f	St. error	R^2
18º15'	9.55	-1.01	1.69	0.01	-2.37	-0.76	3.46	0.19	25º15'	8.30	-0.91	-0.33	-0.06	0.91	-0.08	2.28	0.16
18º30'	10.04	-0.91	1.17	-0.29	-1.94	-0.80	3.45	0.16	25º30'	8.65	-0.98	0.26	-0.58	0.97	-0.10	2.15	0.25
18º45'	9.76	-1.14	1.02	-0.30	-0.96	-0.60	3.24	0.14	25º45'	8.60	-1.02	-0.26	-0.37	0.37	-0.33	1.93	0.27
19º0'	9.52	-1.13	0.84	-0.32	-0.71	-0.51	3.06	0.14	26º0'	8.52	-2.06	-0.60	0.87	0.02	-0.26	2.48	0.31
19º15'	9.52	-1.13	0.84	-0.32	-0.71	-0.51	3.06	0.14	26º15'	8.35	-1.39	-0.83	0.73	-0.76	-0.21	2.51	0.22
19º30'	9.22	-1.11	0.95	-0.47	-0.61	-0.42	3.14	0.14	26º30'	7.91	-1.03	-0.47	0.34	-1.45	-0.01	2.55	0.20
19º45'	8.84	-1.07	0.54	-0.66	-0.42	-0.31	3.10	0.15	26º45'	8.49	-0.72	-0.39	-0.02	-1.31	-0.06	2.69	0.17
20º0'	8.95	-0.82	0.08	-0.42	-0.19	-0.26	2.98	0.09	27º0'	8.92	-0.97	-0.29	-0.07	-1.28	-0.12	2.75	0.17
20º15'	9.06	-0.50	-0.26	-0.48	0.14	-0.25	2.96	0.06	27º15'	9.20	-0.89	-0.48	-0.01	-1.18	-0.12	2.70	0.17
20º30'	8.27	0.11	-0.59	-1.03	1.02	0.01	2.87	0.10	27º30'	9.69	-0.83	-0.71	0.04	-0.97	-0.20	2.67	0.15
20º45'	9.12	-0.33	-0.66	-0.80	0.78	-0.29	2.83	0.10	27º45'	9.92	-0.62	-0.69	-0.14	-0.93	-0.22	2.75	0.14
21º0'	10.66	0.37	-3.02	-1.64	2.18	-0.31	2.44	0.28	28º0'	9.76	-0.40	-0.35	-0.40	-1.29	-0.18	2.78	0.15
21º15'	8.65	-0.18	-1.07	-1.07	0.96	-0.21	2.78	0.14	28º15'	9.65	-0.31	0.10	-1.09	-0.87	-0.19	2.53	0.19
21º30'	8.55	-0.20	-1.15	-0.91	1.01	-0.15	2.69	0.12	28º30'	9.44	-0.88	0.44	-0.81	-1.09	-0.14	2.57	0.22
21º45'	8.49	-0.16	-1.21	-0.82	0.97	-0.16	2.72	0.11	28º45'	9.34	-1.01	0.65	-0.64	-1.29	-0.16	2.56	0.24
22º0'	8.43	-0.31	-1.23	-0.81	1.02	-0.18	2.69	0.13	29º0'	9.25	-1.00	0.73	-0.56	-1.29	-0.18	2.41	0.24
22º15'	8.59	-0.62	-1.11	-1.04	0.87	-0.21	2.81	0.18	29º15'	9.14	-0.95	0.75	-0.79	-1.21	-0.20	2.18	0.30
22º30'	9.71	-0.16	-2.70	-1.84	1.57	-0.28	2.60	0.32	29º30'	8.51	-0.81	0.05	-0.57	-1.04	-0.07	2.45	0.20
22º45'	8.62	-0.80	-1.33	-0.77	0.65	-0.20	2.84	0.17	29º45'	8.84	-0.89	0.13	0.08	-0.59	-0.15	2.35	0.10
23º0'	8.57	-0.49	-1.32	-1.08	0.53	-0.26	2.97	0.15	30º0'	8.59	-0.45	-0.16	-0.31	-0.73	0.10	2.81	0.06
23º15'	8.34	-0.98	-0.21	-1.14	0.24	-0.18	2.88	0.20	30º15'	8.23	-0.48	-0.29	0.32	-0.75	0.16	2.70	0.06
23º30'	7.22	-1.55	1.00	-0.58	-0.16	0.08	2.53	0.28	30º30'	7.85	-0.52	0.53	0.46	-1.03	0.20	2.69	0.07
23º45'	7.14	-1.53	0.92	-0.47	0.02	0.13	2.42	0.29	30º45'	7.72	-0.14	0.43	0.12	-1.41	0.34	2.55	0.12
24º0'	7.61	-1.24	0.00	-0.56	0.38	0.16	2.25	0.26	31º0'	4.86	0.23	-0.08	1.22	-3.84	0.91	3.37	0.36
24º15'	7.76	-1.50	-0.24	-0.41	0.66	0.08	2.22	0.31	31º15'	8.30	-0.91	-0.33	-0.06	0.91	-0.08	2.28	0.16
24º30'	7.97	-1.43	-0.12	0.30	0.70	0.02	2.41	0.20									
24º45'	7.92	-1.39	-0.33	0.26	0.73	0.06	2.37	0.21									
25º0'	7.92	-1.30	-0.07	0.16	0.73	-0.02	2.34	0.20									

MEMORIA FINAL DEL TRABAJO DE FIN DE MÁSTER

1. Descripción de las actividades desarrolladas durante la realización del Trabajo de Fin de Máster

El Trabajo de Fin de Máster (TFM) se ha desarrollado en relación con la asignatura de igual nombre prevista en el Máster Universitario en Oceanografía. El presente trabajo se ha realizado en el grupo de investigación QUIMA, bajo la supervisión del Dr. Melchor González Dávila y la Dra. J. Magdalena Santana Casiano, en la Universidad de Las Palmas de Gran Canaria (ULPGC).

Tras el tratamiento de datos recogidos a través de *Voluntary Observing Ships*(VOS) que operaron a lo largo de la QUIMA-VOS line se procedió a:

- Búsqueda bibliográfica. Para llevar a cabo la consulta se emplearon los recursos telemáticos y en papel proporcionados por la Biblioteca Universitaria de la ULPGC. Para la búsqueda de artículos científicos se consultaron diferentes bases de datos bibliográficas online a las que la Biblioteca Universitaria está adscrita, entre ellas destaca: *SCOPUS, Web of Science, Royal Society of Chemistry* y *ScienceDirect*.

- Profundización en los conocimientos del sistema del dióxido de carbono impartidos durante la asignatura "CO_2 y Acidificación Oceánica". En especial sobre la dinámica de gases en la interfaz atmosfera-océano, las técnicas y parametrizaciones utilizadas para determinar los flujos espacio-temporales sobre una región de alta variabilidad, como es la provincia costera de Sudáfrica.

- Tratamiento de datos, elaboración de gráficos y discusión de la información recopilada.

2. Formación recibida

Para el correcto desarrollo y representación de la información la alumna ha precisado incrementar sus habilidades y conocimientos en los siguientes programas informáticos:

- *Microsoft Excel*. Programa del paquete Office utilización de MACROS específicos elaborados para el estudio de parámetros químicos del océano.

- *SigmaPlot.* Software estadístico y gráfico utilizado para representación de la información.

- *Underway xCO_2 system.* Equipos automatizados de medición de xCO_2 mediante los que se obtiene la información tratada en el presente estudio. El aprendizaje consistió en comprender el funcionamiento de los equipos y participar en su instalación.

- *RStudio.* Software estadístico utilizado para el procesamiento de los datos.

3. Nivel de integración e implicación dentro del departamento y relaciones con el personal

En las diferentes actividades desarrolladas durante los meses de trabajo en el seno del grupo de investigación la alumna se vio involucrada en diferentes ambientes y grupos de trabajo, con diferentes integrantes y funciones. La interacción en el interior de dichos equipos ha sido muy productiva debido no sólo a la diversidad formativa de los componentes sino del buen ambiente establecido. Estas relaciones sociales han amenizado y enriquecido la tarea de la estudiante.

4. Aspectos positivos y negativos más significativos en el desarrollo del TFM

Los aspectos positivos más destacables son la adquisición de nuevos conocimientos y la posibilidad de afianzar los previamente adquiridos a lo largo del Grado.

5. Valoración personal del aprendizaje conseguido a lo largo del TFM

Los conocimientos adquiridos durante el desarrollo del trabajo han permitido ampliar los conocimientos de la oceanografía química, en especial del efecto del cambio climático sobre las regiones costeras, la respuesta de estas regiones y las consecuencias regionales. Al mismo tiempo se hizo patente la importancia de los estudios interdisciplinares en la dinámica oceánica.

Lo más importante en el desarrollo del trabajo fue entender lo que realmente hay detrás de un proyecto de investigación partiendo de las necesidades económicas, los acuerdos con empresas y grupos de investigación, atravesando etapas formativas cada vez más específica, aprendiendo sobre protocolos y tomas de muestras para finalizar con la necesidad de solventar problemas durante el procesamiento de datos, cuando ya no es posible mejorar o cambiar el criterio de muestreo.